MOLECULAR AND CELLULAR BIOLOGY, Sept. 1997, p. 5210–5226 Vol. 17, No. 9
0270-7306/97/$04.00+0

Four Distinct Secretory Pathways Serve Protein Secretion, Cell Surface Growth, and Peroxisome Biogenesis in the Yeast *Yarrowia lipolytica*

VLADIMIR I. TITORENKO,[1] DAVID M. OGRYDZIAK,[2] AND RICHARD A. RACHUBINSKI[1]*

Department of Cell Biology and Anatomy, University of Alberta, Edmonton, Alberta T6G 2H7, Canada,[1] and Department of Food Science and Technology, University of California, Davis, California 95616-8598[2]

Received 14 November 1996/Returned for modification 22 January 1997/Accepted 24 June 1997

We have identified and characterized mutants of the yeast *Yarrowia lipolytica* that are deficient in protein secretion, in the ability to undergo dimorphic transition from the yeast to the mycelial form, and in peroxisome biogenesis. Mutations in the *SEC238*, *SRP54*, *PEX1*, *PEX2*, *PEX6*, and *PEX9* genes affect protein secretion, prevent the exit of the precursor form of alkaline extracellular protease from the endoplasmic reticulum, and compromise peroxisome biogenesis. The mutants *sec238A*, *srp54KO*, *pex2KO*, *pex6KO*, and *pex9KO* are also deficient in the dimorphic transition from the yeast to the mycelial form and are affected in the export of only plasma membrane and cell wall-associated proteins specific for the mycelial form. Mutations in the *SEC238*, *SRP54*, *PEX1*, and *PEX6* genes prevent or significantly delay the exit of two peroxisomal membrane proteins, Pex2p and Pex16p, from the endoplasmic reticulum en route to the peroxisomal membrane. Mutations in the *PEX5*, *PEX16*, and *PEX17* genes, which have previously been shown to be essential for peroxisome biogenesis, affect the export of plasma membrane and cell wall-associated proteins specific for the mycelial form but do not impair exit from the endoplasmic reticulum of either Pex2p and Pex16p or of proteins destined for secretion. Biochemical analyses of these mutants provide evidence for the existence of four distinct secretory pathways that serve to deliver proteins for secretion, plasma membrane and cell wall synthesis during yeast and mycelial modes of growth, and peroxisome biogenesis. At least two of these secretory pathways, which are involved in the export of proteins to the external medium and in the delivery of proteins for assembly of the peroxisomal membrane, diverge at the level of the endoplasmic reticulum.

The secretory pathway of eukaryotic cells consists of a series of morphologically and biochemically distinct membrane-bound compartments. The classical secretory pathway starts with protein translocation into the lumen of the endoplasmic reticulum (ER). From the ER, secretory proteins are transported within a series of vesicles to and through the Golgi complex and are then either delivered to the cell surface or routed to the endosomal-lysosomal (vacuolar) branch of the pathway (32, 43, 53). At all stages of the pathway, intercompartmental transport is initiated by the formation of coated vesicles on the donor compartment, followed by uncoating of vesicle intermediates prior to their fusion with a specific acceptor compartment (47, 52–54). While initial studies suggested the existence of one major pathway of vesicle-mediated protein export to the cell surface through a series of membrane-bound compartments, exceptions to this classical scheme of protein secretion have now been described.

First, not all proteins of either mammalian or yeast cells are delivered to the cell surface via the vesicle-mediated secretory pathway. At least two nonclassical secretory pathways have been demonstrated in the yeast *Saccharomyces cerevisiae* (for a detailed discussion, see references 9 and 10). Second, branching of the pathway for classical vesicle-mediated protein traffic to the cell surface has been shown for some specialized mammalian cells. Divergence occurs at the Golgi complex-to-plasma membrane step that is served by different populations of Golgi complex-derived vesicles (21, 34, 47, 48). The existence of two parallel routes from the Golgi complex to the plasma membrane has also been demonstrated recently for *S. cerevisiae* (22). Branching of the vesicle-mediated secretion pathway can also occur at the level of the ER. Anterograde ER-to-Golgi complex protein traffic in *S. cerevisiae* is mediated by two vesicle populations coated by different protein complexes, COPI and COPII (3, 5). While COPII-coated vesicles are responsible for the transport of the majority of secretory and membrane cargo molecules (5), the role of COPI-coated vesicles remains a matter of debate (3, 5, 44, 54). However, it should be noted that blocking the function of either COPI or COPII affects both protein delivery to the cell envelope and/or external medium and export of material for plasma membrane and cell wall synthesis.

Here, we provide evidence for the existence of four distinct secretory routes in the yeast *Yarrowia lipolytica*. These routes serve protein secretion into the external medium, delivery of proteins for plasma membrane and cell wall synthesis during yeast and mycelial modes of growth, and peroxisome biogenesis. We also show that at least two of these routes, which function in protein secretion and in the delivery of proteins for the assembly of the peroxisomal membrane, diverge at the level of the ER.

MATERIALS AND METHODS

Yeast strains, media, and techniques. The *Y. lipolytica* strains used in this study are listed in Table 1. The mutant *sec238A* and *srp54KO* strains are isogenic to the wild-type *DX547-1A* strain, while the *MCL25*, *pex1-1*, *pex2KO*, *pex5KO*, *pex6KO*, *pex9KO*, *pex16KO*, and *pex17KO* strains are isogenic to the wild-type *E122* strain. The new nomenclature for peroxisome assembly genes and proteins has been used (13). Media, growth conditions, and genetic techniques for *Y. lipolytica* have been described elsewhere (38, 56). Medium components were as follows: YEPD, 1% yeast extract, 2% peptone, and 2% glucose; 2×-YEPD, 2% yeast extract, 4% peptone, and 4% glucose; YEPA, 1% yeast extract, 2% peptone, and 2% sodium

* Corresponding author. Mailing address: Department of Cell Biology and Anatomy, University of Alberta, Medical Sciences Building 5-14, Edmonton, Alberta T6G 2H7, Canada. Phone: (403) 492-9868. Fax: (403) 492-9278. E-mail: rrachubi@anat.med.ualberta.ca.

TABLE 1. *Y. lipolytica* strains

Strain	Genotype	Source or reference
E122	*MATA ura3-302 leu2-270 lys8-11*	18
DX547-1A	*MATA ade1 leu2-270*	D. Ogrydziak
MCL25	*MATA ura3-302 leu2-270 lys8-11 sec14::URA3*	30
sec238A	*MATA ade1 sec238A*	D. Ogrydziak
srp54KO	*MATA ade1 leu2-270 srp54::ADE1*	29
pex1-1	*MATA ura3-302 leu2-270 lys8-11 pex1-1*	This study
pex2KO	*MATA ura3-302 leu2-270 lys8-11 pex2::LEU2*	16
pex5KO	*MATA ura3-302 leu2-270 lys8-11 pex5::LEU2*	56
pex6KO	*MATA ura3-302 leu2-270 lys8-11 pex6::LEU2*	39
pex9KO	*MATA ura3-302 leu2-270 lys8-11 pex9::LEU2*	14
pex16KO	*MATA ura3-302 leu2-270 lys8-11 pex16::URA3*	15
pex17KO	*MATA ura3-302 leu2-270 lys8-11 pex17::URA3*	55

acetate; and YND, 0.67% yeast nitrogen base without amino acids and 2% glucose. YND was supplemented with adenine, uracil, leucine, and lysine each at 50 μg/ml as required.

Isolation of the *sec238A* and *srp54KO* mutants. The *sec238A* mutant was isolated after UV mutagenesis of the *CX161-1B* strain (*MATA ade1*). Mutagenized cells were first screened for the temperature-sensitive production of cell-bound phosphatase by a plate assay for acid phosphatase activity on low-phosphate medium (41). Strains exhibiting levels of extracellular acid phosphatase comparable to those of wild-type cells at 22°C but affected in phosphatase secretion at 32°C were secondarily screened on skim milk plates (41) for temperature-sensitive production of alkaline extracellular protease (AEP). Strains that showed a small or no zone of clearing on skim milk plates at 32°C but which were unimpaired in AEP production at 22°C were selected. Final screening included an immunoblot selection of mutants that accumulated the intracellular 55-kDa precursor form of AEP (pAEP) after temperature shift from 22 to 32°C, in contrast to the wild-type strain, which does not accumulate intracellular pAEP at either temperature. One mutant, the *sec238A* strain, showed decreased efficiency of AEP secretion into the culture supernatant and accumulated intracellular pAEP upon shift from the permissive (22°C) to the restrictive (32°C) temperature in pulse-chase experiments, as described in Results.

The *srp54KO* mutant was constructed by integrative disruption of the *SRP54* gene with the *ADE1* gene of *Y. lipolytica* (29).

The *pex1-1* mutant was originally selected as a peroxisome-deficient strain (38). The *pex2KO* (16), *pex5KO* (56), *pex6KO* (39), *pex9KO* (14), *pex16KO* (15), and *pex17KO* (55) strains were constructed by integrative disruption of genes essential for peroxisome biogenesis as described.

Analysis of protein secretion. Cells, pregrown three times in YEPD medium at 22 or 32°C until an optical density at 600 nm (OD_{600}) of 1.6 to 1.9 were inoculated into YEPD medium at an initial OD_{600} of 0.1. Cells were grown until OD_{600} of 1.7 to 2.0. Phenylmethylsulfonyl fluoride was added to 1 mM to the cell suspension. The cell suspension was subjected to centrifugation in a Beckman JS13.1 rotor at 20,000 × *g* for 15 min at 4°C. The culture supernatant was treated with 10% trichloroacetic acid on ice for 1 h. Precipitated proteins were collected by centrifugation in a Beckman JS13.1 rotor at 20,000 × *g* for 20 min at 4°C, resuspended in 80% (vol/vol) cold acetone, incubated on ice for 30 min, and recollected by centrifugation in a microcentrifuge at 14,000 × *g* for 20 min at 4°C. Protein pellets were dissolved in Laemmli sample buffer and subjected to sodium dodecyl sulfate-polyacrylamide gel electrophoresis (SDS-PAGE), followed either by staining of the gel with Coomassie brilliant blue R-250 or immunoblotting with anti-AEP antibodies after protein transfer to nitrocellulose. The levels of glucose-6-phosphate dehydrogenase (G6PDH) in wild-type and mutant cells were determined by immunoblotting with anti-G6PDH antibodies to ensure the loading of equivalent amounts of culture supernatant from the same number of cells. Whole lysates of cells (20) from 0.5 ml of culture were applied per lane.

Subcellular fractionation and organelle isolation. The initial step in the subcellular fractionation of YEPD-grown *Y. lipolytica* cells was performed as described previously (56) and included the differential centrifugation of lysed and homogenized spheroplasts at 1,000 × *g* for 8 min at 4°C in a Beckman JS13.1 rotor to yield a postnuclear supernatant (PNS). The PNS fraction was further subjected to differential centrifugation at 20,000 × *g* for 30 min at 4°C in a Beckman JS13.1 rotor to yield 20,000 × *g* pellet (20KgP) and supernatant (20KgS) fractions. The 20KgS fraction was further subfractionated by differential centrifugation at 245,000 × *g* for 1 h at 4°C in a Beckman TLA120.2 rotor to yield 245,000 × *g* pellet (245KgP) and supernatant (245KgS) fractions. Protease protection analysis of different subcellular fractions was performed as described elsewhere (58). The separation of organelles, i.e., plasma membrane, mitochondria, ER, Golgi apparatus, and vacuoles, that are present in the 20KgP fraction was performed by isopycnic centrifugation on a discontinuous sucrose (25, 35, 42, and 53% [wt/wt]) gradient in a Beckman VTi50 rotor at 100,000 × *g* for 1 h at 4°C (58).

Cofractionation of ER lumenal (Kar2p and Sls1p) and ER membrane (NADPH-cytochrome *c* reductase [CCR]) proteins with pAEP in the first equilibrium gradient analysis was confirmed by (i) differential centrifugation of the fractions in which these proteins peaked and colocalized at 245,000 × *g* for 1 h at 4°C in a Beckman TLA120.2 rotor, followed by isopycnic centrifugation of the resuspended organellar pellet on a linear (16 to 56% [wt/wt]) sucrose gradient at 100,000 × *g* for 1 h at 4°C in a Beckman VTi50 rotor and by (ii) flotation of the organelles from the peak fractions of the first equilibrium gradient on a two-step sucrose gradient, as described previously (58).

To purify plasma membranes, fraction 7 equilibrating at a density of 1.182 g/cm^3 in the first equilibrium gradient and containing the peak activity of vanadate-sensitive plasma membrane ATPase was subjected to differential centrifugation at 245,000 × g_{max} for 1 h at 4°C in a Beckman TLA120.2 rotor. The resultant pellet was overlaid with 50 mM 2-(*N*-morpholino)ethanesulfonic acid (pH 5.5) containing 1 M sorbitol, and the mixture was placed on ice for 1.5 to 2 h to allow easy resuspension of the pellet. The resuspended pellet was subjected to isopycnic centrifugation on a linear (16 to 56% [wt/wt]) sucrose gradient at 100,000 × *g* for 1 h at 4°C in a Beckman VTi50 rotor. Fraction 6 equilibrating at a density of 1.19 g/cm^3 contained the peak activity of vanadate-sensitive plasma membrane ATPase and was essentially free from contamination (4 to 7%) by other organelles.

High pH extraction of extracellular cell wall-associated proteins was performed as described elsewhere (9).

Radiolabeling and immunoprecipitation. Yeast cultures were grown in YEPD medium at the temperatures indicated. Aliquots of cells were sedimented in a clinical centrifuge, resuspended at a concentration of 2 OD_{600} units/ml in YND medium, and incubated at the temperatures indicated for 30 min. Radiolabeling was performed in the same medium containing L[^{35}S]methionine (ICN Biomedicals, Mississauga, Ontario, Canada) at a concentration of 40 μCi/OD_{600} unit for 1.5 min at the temperatures indicated and chased with an equal volume of 2×-YEPD medium supplemented with 10 mM L-methionine. Samples were taken at the indicated times postchase. Reactions were terminated by the addition of an equal volume of ice-cold 20 mM NaN_3, and cells were immediately separated from the culture supernatant by centrifugation in a microcentrifuge at 20,000 × *g* for 3 min at 4°C. Extracellular radiolabeled proteins were precipitated from the culture supernatant with 10% trichloroacetic acid, as described above. Radiolabeled, cell wall-associated proteins were extracted at high pH and precipitated with 10% trichloroacetic acid as described elsewhere (9). Immunoprecipitation of AEP from culture supernatant (61), cell envelope (9), or crude cell lysate (19) was performed by established methods. Immunoprecipitation of pulse-labeled pAEP, mAEP, Kar2p, and Sec14p from fractions of discontinuous sucrose gradients was performed as described elsewhere (61). Samples were analyzed by SDS-PAGE. Gels were treated with 22.2% 2,5-diphenyloxazole in either dimethylsulfoxide or glacial acetic acid (11), dried, and exposed to preflashed Kodak X-Omat AR X-ray film at −80°C with intensifying screens.

Immunofluorescence microscopy. Double-labeling, indirect immunofluorescence microscopy was performed as described previously (56).

Antibodies. Rabbit polyclonal antibodies to *Y. lipolytica* AEP (31), to *Y. lipolytica* Sls1p (8), and to *Y. lipolytica* Sec14p (30) have been described previously. Anti-Sls1p and anti-Sec14p antibodies were generous gifts of Claude Gaillardin (Institut National Agronomique Paris-Grignon, Thiverval-Grignon, France). Rabbit polyclonal antibodies to *Y. lipolytica* Kar2p were produced against the carboxyl-terminal 180 amino acids of Kar2p expressed as a glutathione *S*-transferase-fusion in *Escherichia coli*. Guinea pig polyclonal antibodies to *Y. lipolytica* Pex2p (16) and to Pex16p (15) have been described. Mouse monoclonal antibody SPA-827 specific for grp78 (BiP) was from StressGen Biotechnologies (Victoria, British Columbia, Canada). Rabbit polyclonal antibody A-9521 specific for *S. cerevisiae* G6PDH was from Sigma (St. Louis, Mo.).

Analytical procedures. The enzymatic activities of cytochrome *c* oxidase (56); NADPH-CCR, α-mannosidase, and vanadate-sensitive plasma membrane ATPase (49); guanosine diphosphatase (1); alkaline phosphatase (57); and extracellular acid phosphatase (41) were determined by established methods. Inorganic phosphate liberated in assays for the activities of guanosine diphosphatase and vanadate-sensitive plasma membrane ATPase was measured as described elsewhere (28). SDS-PAGE (27) and immunoblotting with a semidry electrophoretic transfer system (model ET-20; Tyler Research Instruments, Edmonton, Alberta, Canada) (26) were performed as described. Antigen-antibody complexes were detected by enhanced chemiluminescence (Amersham Life Sciences, Oakville, Ontario, Canada). Immunoblots were quantitated as described elsewhere (56).

RESULTS

Identification of mutants impaired in protein secretion. To determine the effects of the *sec238A* and *srp54KO* mutations on the steady-state levels of proteins secreted, wild-type and mutant strains were grown in YEPD medium at 22 or 32°C until the late exponential phase of growth. Under these conditions, the levels of all secreted proteins were significantly increased and reached steady state in the wild-type strain (data not shown). No differences either in the spectrum of proteins secreted into the culture supernatant or in the intensity of individual protein bands were found between the wild-type strain and the *sec238A* and *srp54KO* mutant strains grown in YEPD at 22°C (Fig. 1A). Neither the *sec238A* nor the *srp54KO* mutation affected the steady-state levels of the 32-kDa mature form of AEP (mAEP) secreted into the culture supernatant or of cell wall-bound extracellular acid phosphatase (AP) at 22°C (Fig. 1A and B). In contrast, most proteins secreted by wild-type cells at 32°C were not secreted, or were secreted to a much lesser extent, by *sec238A* and *srp54KO* cells at 32°C (Fig. 1A). Moreover, at 32°C, the *sec238A* and *srp54KO* mutants secreted four- to fivefold less mAEP or AP vis-à-vis wild-type cells (Fig. 1A and B). The negative effects of the *sec238A* and *srp54KO* mutations on protein secretion at 32°C were even more pronounced in cells grown in YEPA medium, in which both mutants secreted 10- to 12-fold less mAEP and AP compared to the wild-type strain (data not shown).

Because the *sec238A* and *srp54KO* mutations show defects in peroxisome biogenesis (59), we tested the abilities of a set of peroxisome-deficient (*pex*) mutants of *Y. lipolytica* to secrete proteins. Some, but not all, *pex* mutants, i.e., *pex9KO* (14), *pex6KO* (39), *pex2KO* (16), and *pex1-1* (59) strains, were affected in their secretion of all major proteins, including mAEP and AP, compared to wild-type cells (Fig. 1A and B). The defects in protein secretion caused by the *pex9KO*, *pex6KO*, *pex2KO*, and *pex1-1* mutations were observed at both 22°C (data not shown) and 32°C (Fig. 1).

We have confirmed that secretion of both mAEP and AP (Fig. 1) is unaffected by disruption of the *SEC14* gene (30), which encodes a Golgi complex-associated phosphatidylinositol-phosphatidylcholine transfer protein. No differences in the spectrum of the major proteins secreted or in the intensity of individual protein bands were found between the wild type and the *sec14KO* mutant grown in YEPD at both 22°C (data not shown) and 32°C (Fig. 1A).

The *sec238A* and *srp54KO* mutations at 32°C and the *pex9KO*, *pex6KO*, *pex2KO*, and *pex1-1* mutations at both 22 and 32°C affect the rate and efficiency of protein secretion but do not alter the stabilities of secreted proteins or their distributions between the culture supernatant and the cell envelope. At 1 h following a shift of YEPD-grown cells to 32°C, pulse-labeled mAEP appeared in the culture supernatants of wild-type strains at the earliest chase point taken (2 to 2.5 min), and, already by 10 to 20 min of chase, secretion of mAEP into the culture supernatants of wild-type strains was almost complete (Fig. 2A to C and Fig. 3A and B). In contrast, pulse-labeled mAEP appeared in the culture supernatants of the *sec238A*, *srp54KO*, *pex9KO*, *pex6KO*, *pex2KO*, and *pex1-1* strains only after 10 to 40 min of chase. Furthermore, the steady-state levels of mAEP secreted into the medium at the latest chase point taken (120 to 128 min) were 4- to 10-fold less in the mutant strains compared to the wild-type strain (Fig. 2A to C and Fig. 3A and B). Similar to their effects on the secretion of mAEP, the *sec238A*, *srp54KO*, *pex9KO*, *pex6KO*, *pex2KO*, and *pex1-1* mutations at 32°C also affected the rate and efficiency of secretion of all other proteins secreted by the wild-type strains

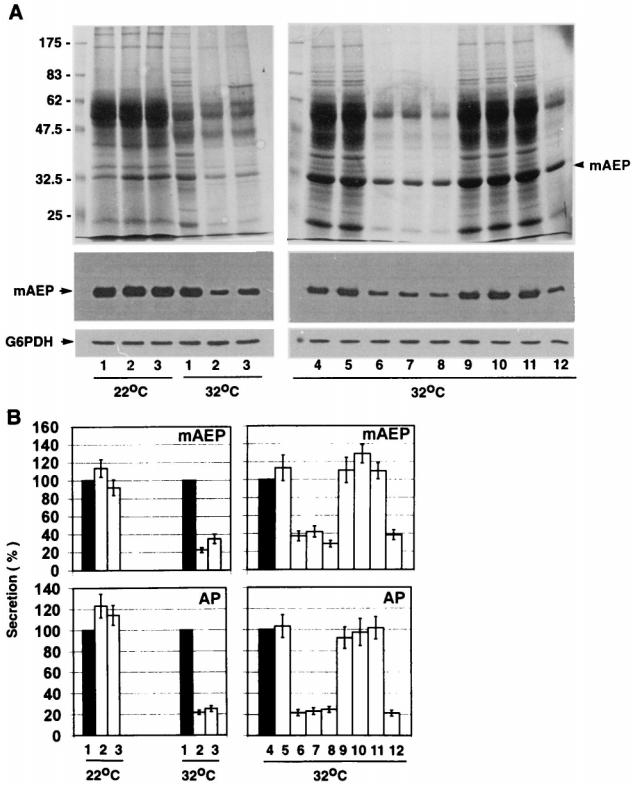

FIG. 1. The *sec238A*, *srp54KO*, *pex9KO*, *pex6KO*, *pex2KO*, and *pex1-1* mutations cause the steady-state levels of secreted proteins to decrease. (A) Cells of the wild-type *DX547-1A* (lane 1) and *E122* (lane 4) strains and of the mutant *sec238A* (lane 2), *srp54KO* (lane 3), *sec14KO* (lane 5), *pex9KO* (lane 6), *pex6KO* (lane 7), *pex2KO* (lane 8), *pex5KO* (lane 9), *pex16KO* (lane 10), *pex17KO* (lane 11), and *pex1-1* (lane 12) strains were grown in YEPD medium at either 22 or 32°C. Culture supernatants were processed for analysis of the spectra of secreted proteins (top panels). The equivalent of 25 ml of culture supernatant per lane was applied. Gels were stained with Coomassie brilliant blue R-250. Numbers at left indicate the migration of molecular mass standards (in kilodaltons). The position of mAEP is indicated by an arrowhead. Culture supernatants were processed for the analysis of secreted mAEP levels (middle panels). Protein from 0.5 ml of culture supernatant was applied to each lane. The blots were probed with anti-AEP antibodies. The levels of G6PDH in whole-cell lysates of the wild-type and mutant strains were determined so as to ensure the loading of equivalent amounts of culture supernatants from the same number of cells onto gels (bottom panels). The lysate of cells from 0.5 ml of culture was applied to each lane. The blots were probed with anti-G6PDH antibodies. (B) Determination of the levels of mAEP and AP secreted into the culture supernatant or into the cell envelope, respectively. For mAEP, blots in panel A (middle panels) were quantitated by densitometry. Values for the densitometric signals of mAEP and for the specific activities of extracellular AP in the culture supernatants or the cell envelopes, respectively, of mutant strains are relative to the corresponding values of the isogenic wild-type strain grown at the same temperature. All values reported are the means ± standard deviations for three independent experiments.

(Fig. 2A and 3A). While the *sec238A* and *srp54KO* mutations affected the rate and efficiency of protein secretion only at 32°C (Fig. 2) but not at 22°C (data not shown), the *pex9KO*, *pex6KO*, *pex2KO*, and *pex1-1* mutations caused similar effects on protein secretion at 32°C (Fig. 3) and 22°C (data not shown).

None of the mutations tested decreased the stability of pulse-labeled proteins, including that of mAEP, which was secreted into the culture supernatant and incubated for 2 h (the approximate length of one doubling time of cultures grown in YEPD medium) at either 22 or 32°C (Fig. 2D and 3C). Furthermore, no differences in the distribution of mAEP

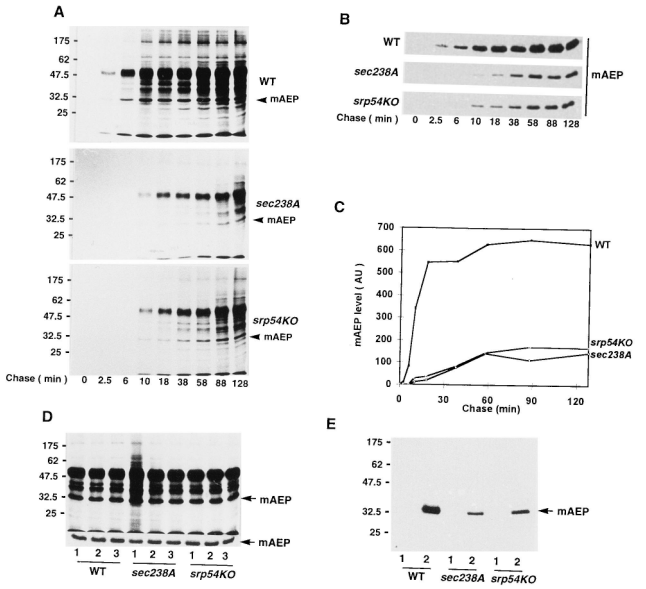

FIG. 2. The *sec238A* and *srp54KO* mutations affect the efficiency of protein secretion but not the stabilities of secreted proteins or their distributions between the culture supernatant and the cell envelope. (A to C) Cells of the wild-type *DX547-1A* strain and the mutant *sec238A* and *srp54KO* strains were grown in YEPD at 22°C until an OD_{600} of 1.0 to 1.2, shifted to 32°C for 1 h, pulse-labeled at 32°C for 1.5 min with L-[^{35}S]methionine, and subjected to chase with unlabeled methionine. Samples were taken at the indicated times postchase, and culture supernatants were processed for analysis of the spectra of secreted proteins (A) or for immunoprecipitation of mAEP (B). Samples were resolved by SDS-PAGE and visualized after fluorography for 24 h. (C) Fluorograms in panel B were quantitated by densitometry. (D) Strains were grown in YEPD medium at 22°C until an OD_{600} of 1.0 to 1.2, pulse-labeled at 22°C for 1.5 min with L-[^{35}S]methionine, and subjected to a 30-min chase with unlabeled methionine. Cell cultures from each strain were separated into three equal aliquots. One aliquot was frozen at −80°C as a control sample (lanes 1) and a second was kept for 2 h at 22°C (lanes 2), while the third was incubated for 2 h at 32°C (lanes 3). Culture supernatants were processed for analysis of the spectra of secreted proteins (upper panel) or for immunoprecipitation of mAEP (lower panel). Samples were resolved by SDS-PAGE and visualized after fluorography for 24 h. (E) Strains were grown in YEPD at 22°C, shifted for 1 h at 32°C, pulse-labeled at 32°C for 1.5 min with L-[^{35}S]methionine, and subjected to a 38-min chase with unlabeled methionine. AEP extracted from the cell envelope (lanes 1) or secreted into the culture supernatant (lanes 2) was immunoprecipitated. Immunoprecipitates were resolved by SDS-PAGE and visualized after fluorography for 24 h. Numbers to the left in (panels A, D, and E) indicate the migration of molecular mass standards (in kilodaltons). WT, wild type.

between the culture supernatant and the cell envelope were observed between wild-type and protein secretion-deficient mutant strains at either 22°C (data not shown) or 32°C (Fig. 2E and 3D).

Exit of the AEP precursor from and translocation of some proteins into the ER are affected in protein secretion-deficient mutants. AEP is synthesized as a 53-kDa preproprotein with an amino-terminal signal sequence and a prodomain upstream from the mature segment of the protein (18, 31). The earliest precursor detected in wild-type cells, the 55-kDa pAEP, lacks its signal peptide, contains N-linked sugars, and is localized to the lumen of the ER (8, 31). The cleavage of the prodomain by a Kex2p-like endoprotease in a late Golgi compartment yields the 32-kDa mature form (mAEP), which is secreted (8, 31). Using pulse-labeling and immunoprecipitation of intracellular forms of AEP after temperature shift to 32°C, we compared the rate of conversion of pAEP to mAEP, reflecting the rate of pAEP transit from the ER to a late Golgi compartment (8, 30, 31), in the wild-type strain to that in protein secretion-deficient mutants. In wild-type cells, 45 to 54% of pulse-labeled pAEP was converted to mAEP by 2 to 2.5 min of chase, and maturation was complete by 10 min of chase (Fig. 4A and B). In contrast, in protein secretion-deficient mutants at 32°C, most prelabeled pAEP (65 to 74% of the initial levels in *sec238A* and *srp54KO* strains and 81 to 89% of the initial levels in *pex9KO*, *pex6KO*, *pex2KO*, and *pex1-1* strains) was detected as an intracellular form even by 120 to 128 min of chase (Fig. 4A and B). Immunoprecipitation of prelabeled and chased pAEP and mAEP, of the ER lumenal protein (Kar2p), and of the Golgi marker protein (Sec14p) from fractions of discontinuous sucrose density gradients of the 20KgP subcellular fractions showed cofractionation of immunoprecipitated pAEP and Kar2p in the wild-type strain grown at 32°C, as well as in the *sec238A* mutant strain grown at 32 or 22°C (Fig. 4C). Immunoprecipitated Kar2p of the wild-type strain at 32°C and of the *sec238A* mutant at 22°C peaked in fraction 12 with a density of 1.14 g/cm^3. Immunoprecipitated Kar2p equilibrated at a density of 1.11 g/cm^3 (fraction 14) for the *sec238A* mutant grown at 32°C, i.e., at the temperature restrictive for secretion (Fig. 4C). Therefore, the *sec238A* mutant at 32°C was altered in the buoyant density of its ER (see also Fig. 6). The distribution of immunoprecipitated mAEP around peak fraction 16 of the wild-type strain at 32°C and of the *sec238A* mutant at 22°C coincided with the distribution of the Golgi marker Sec14p (Fig. 4C). No prelabeled mAEP was detected by immunoprecipitation from gradient fractions of the 20KgP of the *sec238A* mutant grown at 32°C (Fig. 4C). In the wild-type strain at 32°C and in the *sec238A* mutant at 22 or 32°C, immunoprecipitated intracellular pAEP cofractionated only with the ER marker, Kar2p, but not with markers of the Golgi complex (Sec14p [Fig. 4C]), plasma membrane, mitochondria, or vacuoles (see Fig. 6 for the distribution of marker proteins of different organelles in the fractions of a gradient similar to that shown in Fig. 4C). In contrast, in the wild-type strain at 32°C and in the *sec238A* mutant at 22°C, immunoprecipitated intracellular mAEP cofractionated only with the Golgi marker Sec14p (Fig. 4C) but not with the ER marker Kar2p (Fig. 4C) or with marker proteins of plasma membrane, mitochondria, or vacuoles (see Fig. 6 for the distribution of marker proteins for these organelles in a gradient similar to that shown in Fig. 4C). The rate of transit of mAEP from a late Golgi compartment to the extracellular medium was quite rapid in wild-type cells at 32°C, since this intracellular form appeared by 2 to 2.5 min of chase and could not be detected by 18 to 20 min of chase (Fig. 4A and B). No intracellular pulse-labeled mAEP was detected in cells of all protein secretion-deficient mutants at 32°C (Fig. 4A and B), suggesting that the transit of mAEP from a late Golgi compartment to the extracellular medium is not rate limiting for mAEP secretion by mutant cells. While the *sec238A* and *srp54KO* mutations affect the rate and efficiency of conversion of intracellular pAEP to mAEP only at 32°C (Fig. 4A and B) but not at 22°C (data not shown), the *pex9KO*, *pex6KO*, *pex2KO*, and *pex1-1* mutations have similar effects on pAEP-to-mAEP conversion at both 32°C (Fig. 4A and B) and 22°C (data not shown). Therefore, the *sec238A* and *srp54KO* mutations at 32°C and the *pex9KO*, *pex6KO*, *pex2KO*, and *pex1-1* mutations at both 22 and 32°C affect the exit of pAEP from the ER, while the rate of transit of mAEP from a late Golgi compartment to the extracellular medium is not significantly impaired by any of these mutations.

The results of subcellular fractionation of wild-type and mutant strains are in agreement with this conclusion. Both the *sec238A* and *srp54KO* strains accumulated intracellular pAEP only at 32°C, the temperature restrictive for the conversion of intracellular pAEP to mAEP and for protein secretion (Fig. 5A). The *pex9KO*, *pex6KO*, *pex2KO*, and *pex1-1* strains accu-

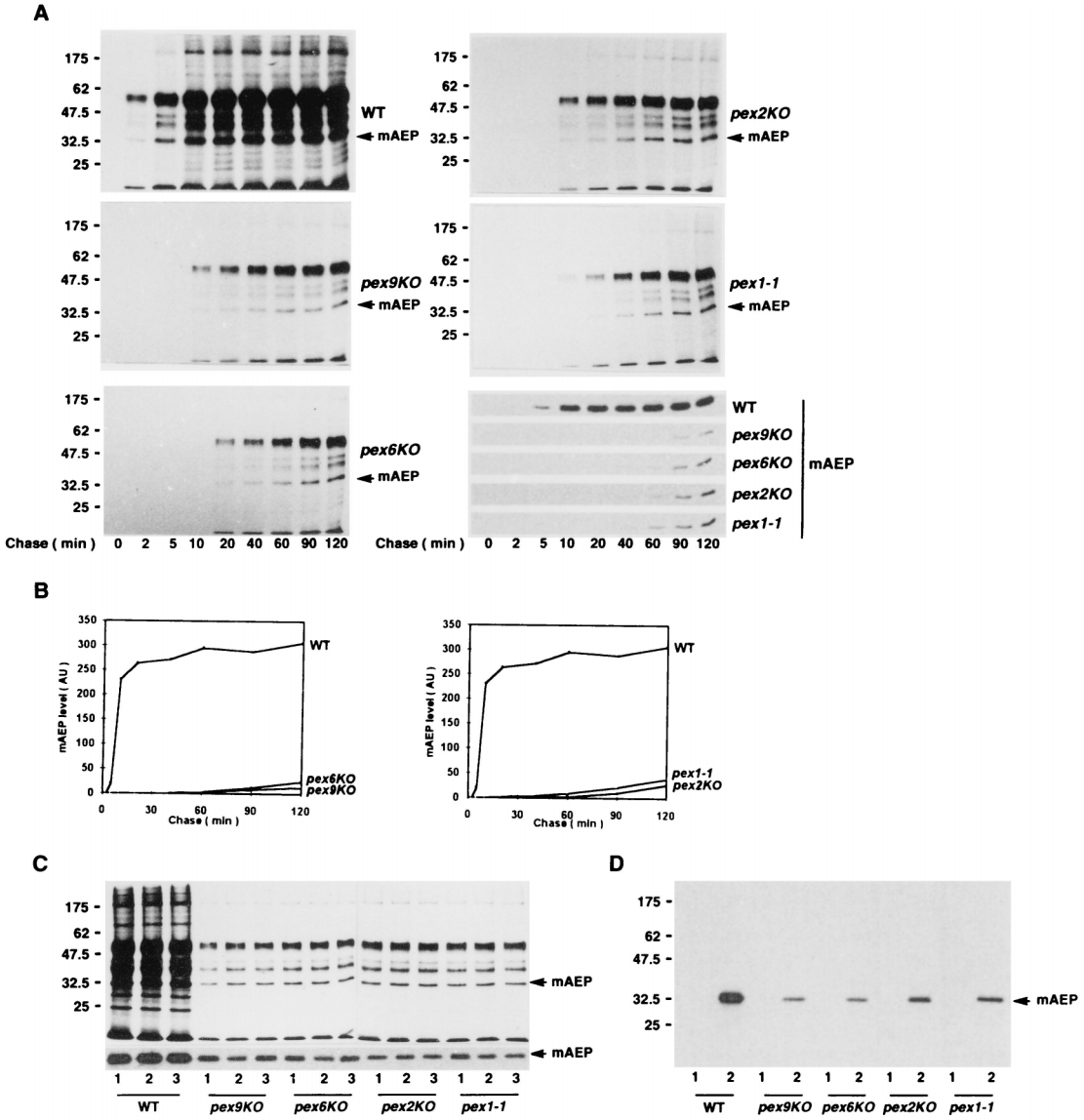

FIG. 3. The *pex9KO*, *pex6KO*, *pex2KO*, and *pex1-1* mutations affect the efficiency of protein secretion but not the stabilities of secreted proteins or their distributions between the culture supernatant and the cell envelope. Cells of the wild-type *E122* strain and the mutant *pex9KO*, *pex6KO*, *pex2KO*, and *pex1-1* strains were grown in YEPD medium at 32°C until an OD_{600} of 1.0 to 1.2, pulse-labeled at 32°C with L-[^{35}S]methionine, and subjected to chase with unlabeled methionine. (A) Samples were taken at the indicated times postchase, and culture supernatants were processed for analysis of the spectrum of secreted proteins or for immunoprecipitation of mAEP. Samples were resolved by SDS-PAGE and visualized after fluorography for 24 h. (B) Fluorograms in panel A showing the amounts of immunoprecipitated mAEP were quantitated by densitometry. (C) Cells were grown in YEPD medium at 22°C until an OD_{600} of 1.0 to 1.2, pulse-labeled at 22°C for 1.5 min with L-[^{35}S]methionine, and subjected to a 120-min chase with unlabeled methionine. Cell cultures from each strain were separated into three equal aliquots. One aliquot was frozen at −80°C as a control and a second was kept for 2 h at 22°C, while the third was incubated for 2 h at 32°C. Culture supernatants before (lanes 1) and after the 2-h incubation at 22°C (lanes 2) or 32°C (lanes 3) were processed for analysis of the spectrum of secreted proteins or for immunoprecipitation of mAEP. Samples were resolved by SDS-PAGE and visualized after fluorography for 24 h. The upper panel shows the spectra of secreted proteins, while the lower panel shows the amounts of immunoprecipitated mAEP. (D) Strains were grown in YEPD medium at 32°C until OD_{600} of 1.0 to 1.2, pulse-labeled at 32°C for 1.5 min with L-[^{35}S]methionine, and subjected to a 120-min chase with unlabeled methionine. mAEP extracted from the cell envelope (lanes 1) or mAEP secreted into the culture supernatant (lanes 2) was immunoprecipitated. Immunoprecipitates were resolved by SDS-PAGE and visualized after fluorography for 36 h. Numbers at left in panels A, C, and D indicate the migration of molecular mass standards (in kilodaltons). WT, wild type.

mulated intracellular pAEP at both 22°C (data not shown) and 32°C (Fig. 5A). In all strains, pAEP accumulated in pelletable fractions (20KgP and 245KgP) but not in the cytosolic fraction (245KgS) (Fig. 5A). Protease protection experiments (Fig. 5B) revealed that pelletable pAEP was resistant to trypsin digestion in the absence of the detergent Triton X-100, demonstrating that pAEP was present in a membrane-protected form in all protein secretion-deficient mutants.

Further subfractionation of the 20KgP by isopycnic centrifugation on a discontinuous sucrose density gradient demonstrated the cofractionation of pAEP with two ER lumenal proteins, Kar2p and Sls1p (Fig. 6A), and with the ER membrane protein NADPH-CCR (CCR) (Fig. 6B). Cofractionation of ER protein markers and pAEP was confirmed by a second isopycnic centrifugation of the peak fractions from the first isopycnic centrifugation experiment on a linear sucrose density gradient and by flotation on a two-step sucrose gradient (data not shown). Moreover, the distribution of pAEP

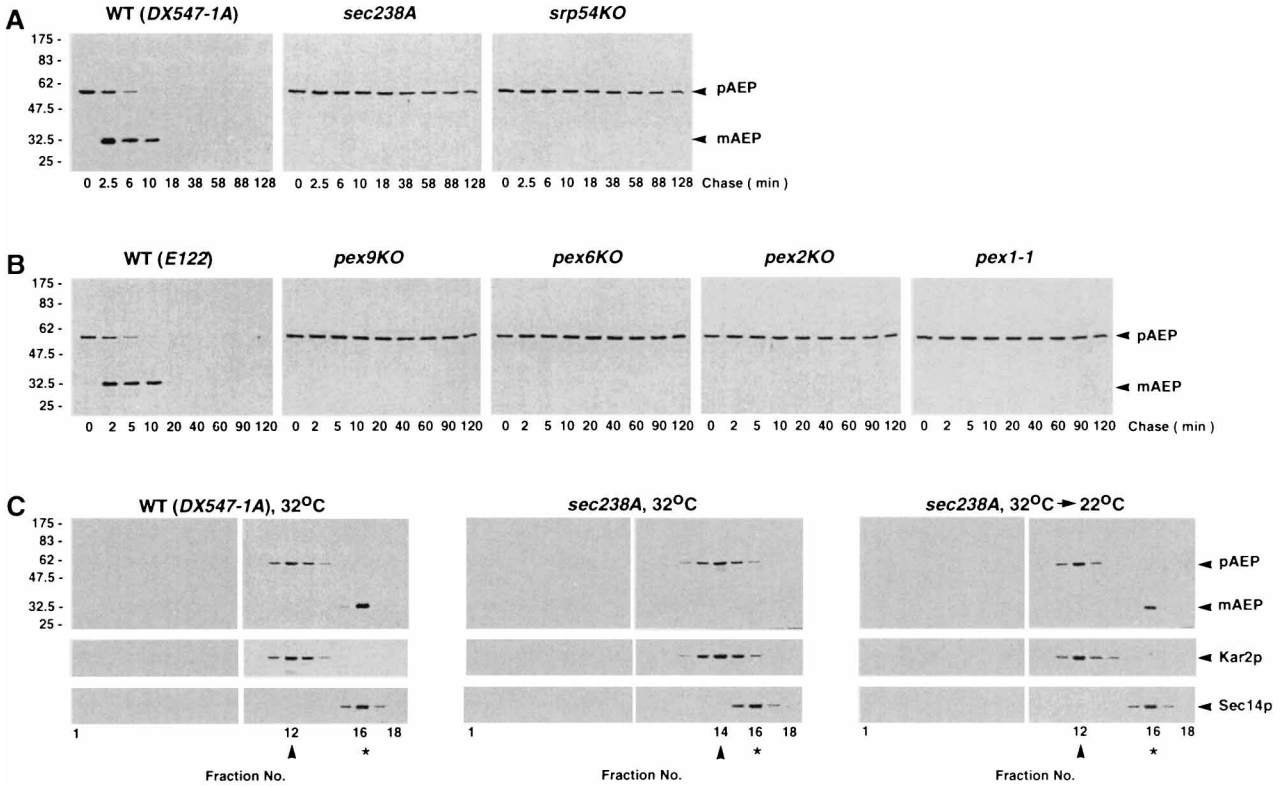

FIG. 4. The *sec238A*, *srp54KO*, *pex9KO*, *pex6KO*, *pex2KO*, and *pex1-1* mutations affect the conversion of intracellular, ER-associated pAEP to Golgi complex-associated mAEP and cause the accumulation of intracellular pAEP in the ER. (A and B) Wild-type and mutant strains were grown in YEPD medium at 22°C until an OD_{600} of 1.0 to 1.2, shifted to 32°C for 1 h, pulse-labeled at 32°C for 1.5 min with L-[^{35}S]methionine, and chased with unlabeled methionine. Samples were taken at the indicated times postchase. Cell-associated pAEP and mAEP were immunoprecipitated from cell lysates with anti-AEP antibodies. Immunoprecipitates were resolved by SDS-PAGE and visualized by fluorography for 60 h. (C) The wild-type *DX547-1A* strain and mutant *sec238A* strain were grown in YEPD medium at 32°C until an OD_{600} of 1.0 or 1.3, respectively. The *sec238A* culture was divided into two equal aliquots. The first aliquot was kept for 1 h at 32°C, while the second was incubated for 1 h at 22°C. Wild-type cells were kept for 1 h at 32°C. Cells were pulse-labeled either at 32°C (wild-type cells and the first aliquot of the *sec238A* mutant) or at 22°C (the second aliquot of the *sec238A* mutant) for 1.5 min with L-[^{35}S]methionine and subjected to a 2.5-min chase with unlabeled methionine. Cells were subjected to subcellular fractionation, and the 20KgP fractions were further fractionated by isopycnic centrifugation on discontinuous sucrose density gradients. pAEP, mAEP, Kar2p, and Sec14p were immunoprecipitated from gradient fractions. Immunoprecipitates were resolved by SDS-PAGE and visualized by fluorography for 42 h. Arrowheads, peak fractions in which immunoprecipitated Kar2p was localized; asterisks, peak fractions in which immunoprecipitated Sec14p was recovered. The positions of the 55-kDa precursor form (pAEP) and of the 32-kDa mature form (mAEP) of AEP, Kar2p, and Sec14p are indicated at right. Numbers at left indicate the migration of molecular mass standards (in kilodaltons). WT, wild type.

around the peak fraction 14 of discontinuous sucrose density gradients of the 20KgPs of the *sec238A* and *srp54KO* strains grown at 32°C coincided only with the distribution of ER lumenal and membrane proteins (Kar2p, Sls1p, and NADPH-CCR) but not with the distributions of enzyme activity of the plasma membrane marker vanadate-sensitive ATPase, of the mitochondrial marker cytochrome *c* oxidase, of the Golgi markers Sec14p and guanosine diphosphatase, or of the vacuolar marker alkaline phosphatase (Fig. 6). In the *pex9KO*, *pex6KO*, *pex2KO*, and *pex1-1* strains at both 32°C (Fig. 6A) and 22°C (data not shown), pAEP accumulated intracellularly and cofractionated in fraction 14 with ER lumenal and membrane proteins but not with markers of the Golgi complex (Fig. 6A [Sec14p]; data for guanosine diphosphatase not shown), plasma membrane, mitochondria, or vacuoles (data not shown). Therefore, in all protein secretion-deficient mutants, pAEP accumulated in the ER at the temperature restrictive for protein secretion and did not associate with any other organelle.

The localization of pAEP to the ER in protein secretion-deficient mutants was confirmed by double-labeling indirect immunofluorescence. The fluorescence patterns generated by anti-rat BiP and anti-*Y. lipolytica* AEP antibodies in *sec238A*, *srp54KO*, and *pex1-1* cells (Fig. 7), as well as in *pex9KO*, *pex6KO*, or *pex2KO* cells (data not shown), which were grown at the temperatures restrictive for protein secretion, were superimposable and showed bright staining of the perinuclear region and cell periphery and, occasionally, of filamentous extensions into the cytosol. These fluorescence patterns are characteristic of the ER (46, 51). The fluorescence patterns generated by anti-rat BiP, anti-*Y. lipolytica* hKar2p, and anti-*Y. lipolytica* Sls1p antibodies were also superimposable, demonstrating that anti-rat BiP antibodies recognize ER protein(s) in *Y. lipolytica* cells (data not shown). In contrast, anti-*Y. lipolytica* Sec14p antibodies (Fig. 7) yielded a bright punctate staining frequently clustering in a perinuclear region of the cell and characteristic of the Golgi complex (30). These structures failed to colocalize with the ER in double-labeling indirect immunofluorescence experiments with anti-Sec14p and anti-BiP antibodies (data not shown). Therefore, the results of indirect immunofluorescence microscopy are in agreement with those of pulse-chase and immunoprecipitation analysis of subcellular fractions and demonstrate that intracellular pAEP is localized to the ER but is not associated with the Golgi complex in protein secretion-deficient mutants.

The *sec238A* and *srp54KO* mutants at the restrictive temper-

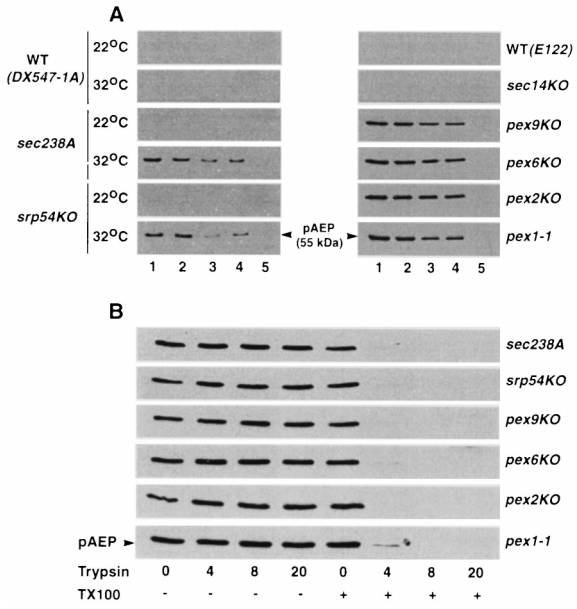

FIG. 5. Protein secretion-deficient mutants accumulate intracellular pAEP in a membrane-enclosed form. (A) Wild-type and mutant strains were grown in YEPD medium at 22 or 32°C and then subjected to subcellular fractionation. Equal fractions (1% of the total volume) of the PNS (lanes 1), 20KgP (lanes 2), 20KgS (lanes 3), 245KgP (lanes 4), and 245KgS (lanes 5) were analyzed by immunoblotting with anti-AEP antibodies. (B) Equal fractions (1% of the total volume) of PNS isolated from mutant cells grown in YEPD medium at 32°C were incubated with 0, 4, 8, and 20 μg of trypsin/100 μg of protein in the absence (−) or presence (+) of 0.5% (vol/vol) Triton X-100 for 40 min on ice. Reactions were terminated by addition of trichloroacetic acid to 10%. Equal fractions of samples were subjected to immunoblot analysis with anti-AEP antibodies. The position of the 55-kDa precursor of AEP (pAEP) is indicated by an arrowhead. WT, wild type.

ature (32°C) and the *pex9KO*, *pex6KO*, *pex2KO*, and *pex1-1* mutants at both 22 and 32°C showed an accumulation of the 75-kDa precursor form (pKar2p) of Kar2p in the 245KgS (cytosolic) fraction (Fig. 8A). Unlike the mature 73-kDa form of Kar2p, pKar2p was susceptible to degradation by externally added trypsin in the absence of detergent (Fig. 8A). Therefore, the translocation of Kar2p into the lumen of the ER was affected by all mutations causing a deficiency in protein secretion. It should be noted that although substantial amounts of pKar2p accumulated in the cytosol of the *sec238A*, *srp54KO*, *pex9KO*, *pex6KO*, *pex2KO*, and *pex1-1* mutants grown at the temperatures restrictive for secretion, no significant differences in the levels of the mature, ER-associated form of Kar2p were observed between the wild-type and mutant strains (Fig. 8A; compare the levels of the mature form of Kar2p in the 245KgP fractions of the wild-type and mutant strains). The *pex2KO* mutation also caused a defect in the translocation of another protein, Sls1p, into the lumen of the ER and led to the accumulation of the 58-kDa precursor (pSls1p) form of Sls1p in the 245KgS fraction (Fig. 8B). Again, pSls1p, but not mature Sls1p, was susceptible to degradation by externally added trypsin in the absence of detergent (Fig. 8C).

The *sec238A* and *srp54KO* mutants at 32°C and the *pex9KO*, *pex6KO*, *pex2KO*, and *pex1-1* mutants at both 22 and 32°C were not only affected in the exit of pAEP from the ER and in the translocation of some proteins into the ER but were also altered in the buoyant density of their ER elements. Upon isopycnic centrifugation of the 20KgP fraction, the ER proteins Kar2p, Sls1p, and CCR of the two-wild type strains (*DX547-1A* and *E122*) peaked at densities of 1.14 g/cm^3 (fraction 12) and 1.17 g/cm^3 (fraction 10), respectively (Fig. 6). In contrast, these ER marker proteins equilibrated at a density of 1.11 g/cm^3 (fraction 14) for the *sec238A* and *srp54KO* strains (isogenic to the *DX547-1A* strain) and for the *pex9KO*, *pex6KO*, *pex2KO*, and *pex1-1* strains (isogenic to the *E122* strain) (Fig. 6).

Some but not all protein secretion-deficient mutants transiently or permanently accumulate the proteins Pex2p and Pex16p in the ER. In wild-type *Y. lipolytica* cells grown in oleic acid-containing medium, Pex2p and Pex16p are, correspondingly, integral (16) and peripheral (15) peroxisomal membrane proteins that are essential for peroxisome biogenesis. Indirect immunofluorescence microscopy of wild-type and protein secretion-deficient strains grown in YEPD at 22°C and then shifted to 32°C for 1 or 4 h with anti-Pex2p (Fig. 9) and anti-Pex16p (Fig. 10) antibodies yielded a punctate pattern of staining characteristic of peroxisomes at both temperatures. In wild-type cells, these punctate structures failed to colocalize with the ER, as judged by double labeling immunofluorescence with anti-Pex2p and anti-Kar2p (Fig. 9) or anti-Pex16p and anti-Kar2p (Fig. 10) antibodies. In contrast, the fluorescence patterns generated by anti-Pex2p and anti-Kar2p (Fig. 9) or by anti-Pex16p and anti-Kar2p (Fig. 10) antibodies in *pex6KO* and *pex1-1* cells either grown at 22°C or shifted to 32°C were superimposable and showed staining characteristic of the ER (cf. Fig. 7). The fluorescence patterns generated by anti-Pex2p and anti-Kar2p (Fig. 9) and by anti-Pex16p and anti-Kar2p (Fig. 10) antibodies in *sec238A* cells grown at 22°C were similar to those seen for wild-type cells. However, a 1-h shift of *sec238A* cells to 32°C, the temperature restrictive for the exit of AEP from the ER and for protein secretion, caused the localization of a significant fraction of both Pex2p (Fig. 9) and Pex16p (Fig. 10) to the ER. The association of both proteins with the ER was transient, since after incubation of *sec238A* cells for 4 h at 32°C, both anti-Pex2p (Fig. 9) and anti-Pex16p (Fig. 10) antibodies yielded a punctate pattern of staining characteristic of peroxisomes. A similar transient association of Pex2p and Pex16p with the ER was observed in *srp54KO* cells shifted from 22 to 32°C (data not shown). The fluorescence patterns generated by anti-Pex2p and anti-Pex16p antibodies in *pex9KO* cells and by anti-Pex16p antibodies in *pex2KO* cells grown at either temperature were quite similar to that observed in wild-type cells and showed no association of Pex2p and Pex16p with the ER (data not shown). Our data suggest that in the wild-type cells, the transit of at least two proteins, Pex2p and Pex16p, to the peroxisomal membrane occurs via the ER. The exit of both peroxisomal membrane proteins from the ER is prevented by the *pex6KO* and *pex1-1* mutations and is significantly delayed by the *sec238A* and *srp54KO* mutations. Not all components essential for the exit of pAEP from the ER are also required for the exit of Pex2p and Pex16p. While the *pex9KO* and *pex2KO* mutations affect the exit of pAEP from the ER, neither prevents the trafficking of Pex16p and, in the case of the *pex9KO* mutation, of Pex2p to the peroxisomal membrane via the ER. Moreover, while pAEP is continuously associated with the ER in *sec238A* and *srp54KO* cells grown at the restrictive temperature, the trafficking of Pex2p and Pex16p to the peroxisomal membrane via the ER is only significantly delayed but not blocked in these cells.

Effects of mutations causing defects in protein secretion on growth in YEPD and on the dimorphic transition from the yeast to the mycelial form. The *sec238A* and *srp54KO* strains were not affected in growth in YEPD medium at 22 or 32°C, compared to the wild-type *DX547-1A* strain (Fig. 11). In addition, no differences in growth rates at either temperature were observed for the wild-type *E122* strain and its isogenic mutant

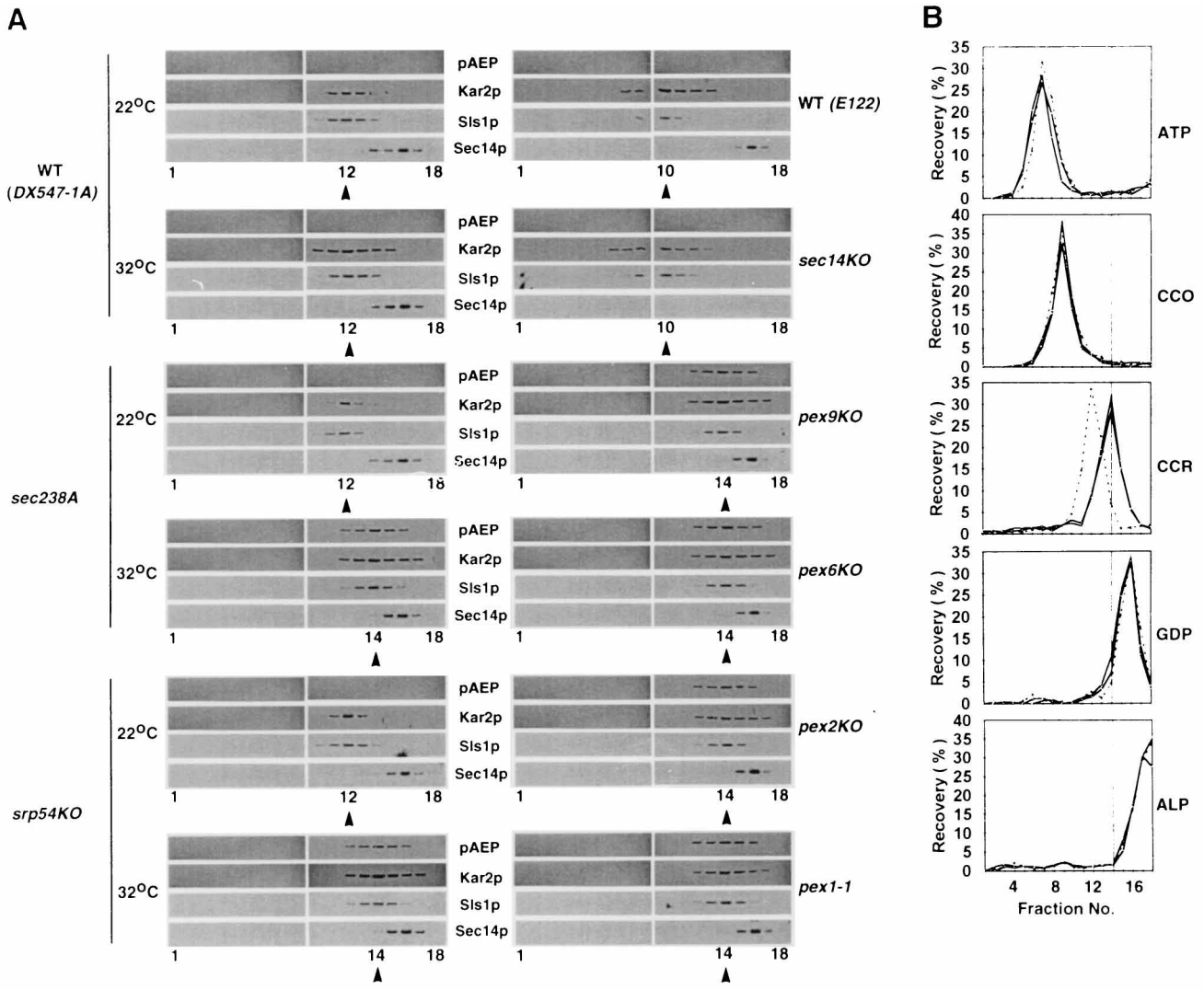

FIG. 6. pAEP in protein secretion-deficient mutants is localized to ER elements having altered buoyant density. Wild-type (WT) and mutant strains were grown in YEPD medium at 22 or 32°C. Cells were subjected to subcellular fractionation, and the 20KgP fraction of each strain was further fractionated by isopycnic centrifugation in a discontinuous sucrose density gradient. (A) Equal volumes (2% of the total fraction volume for anti-Kar2p and anti-Sls1p, 5% for anti-Sec14p, and 10% for anti-AEP antibodies) of gradient fractions were analyzed by immunoblotting. Arrowhead, peak fractions in which Kar2p, Sls1p, and pAEP of protein secretion-deficient mutants colocalized. (B) Percentage recovery of vanadate-sensitive ATPase (ATP), cytochrome *c* oxidase (CCO), NADPH-CCR (CCR), guanosine diphosphatase (GDP), and alkaline phosphatase (ALP) in gradient fractions of the wild-type (dotted line [■]), *sec238A* (solid line [□]), and *srp54KO* (solid line [x]) strains grown in YEPD medium at 32°C. Vertical lines in panel B indicate the peak fraction 14 in which Kar2p, Sls1p, CCR, and pAEP of the *sec238A* and *srp54KO* mutants grown at 32°C colocalized.

sec14KO, *pex9KO*, *pex6KO*, *pex2KO*, and *pex1-1* strains (data not shown).

The dimorphic transition from the yeast to the mycelial form is developmentally regulated in *Y. lipolytica* (50). We compared the cell morphologies of the wild-type strains and protein secretion-deficient mutants during growth in YEPD medium at 22 or 32°C. No dimorphic transition was observed for wild-type or mutant cells grown at 22°C (Fig. 12 [wild-type *DX547-1A* strain and mutant *sec238A* and *srp54KO* strains]; data for the wild-type *E122* strain and its isogenic mutants not shown). Upon entering early stationary phase, wild-type cells grown at 32°C underwent dimorphic transition (Fig. 12). In contrast, the *sec238A*, *srp54KO*, *pex9KO*, *pex6KO*, and *pex2KO* mutants did not undergo transition at 32°C (Fig. 12), even after prolonged (up to 72 h) incubation. This mutant phenotype is quite similar to that observed for the *sec14KO* mutant (Fig. 12) (30). However, not all protein secretion-deficient mutants were affected in their transition from the yeast to the mycelial form. No effect of the *pex1-1* mutation on the transition was observed upon growth at 32°C (Fig. 12).

The mutant *pex5KO*, *pex16KO*, and *pex17KO* strains did not undergo dimorphic transition when grown at 32°C (Fig. 12). These mutants were unaffected in protein secretion (Fig. 1), exit of pAEP, Pex2p and Pex16p from the ER, translocation of Kar2p and Sls1p into the ER, and growth at either 22 or 32°C (data not shown).

Effects of mutations affecting protein secretion on the rate and efficiency of delivery of plasma membrane and cell wall-associated proteins. A pulse-chase regimen was used to monitor and compare the rates and efficiencies of delivery of proteins to the plasma membrane and cell envelope in wild-type and protein secretion-deficient mutant strains. Cells grown in

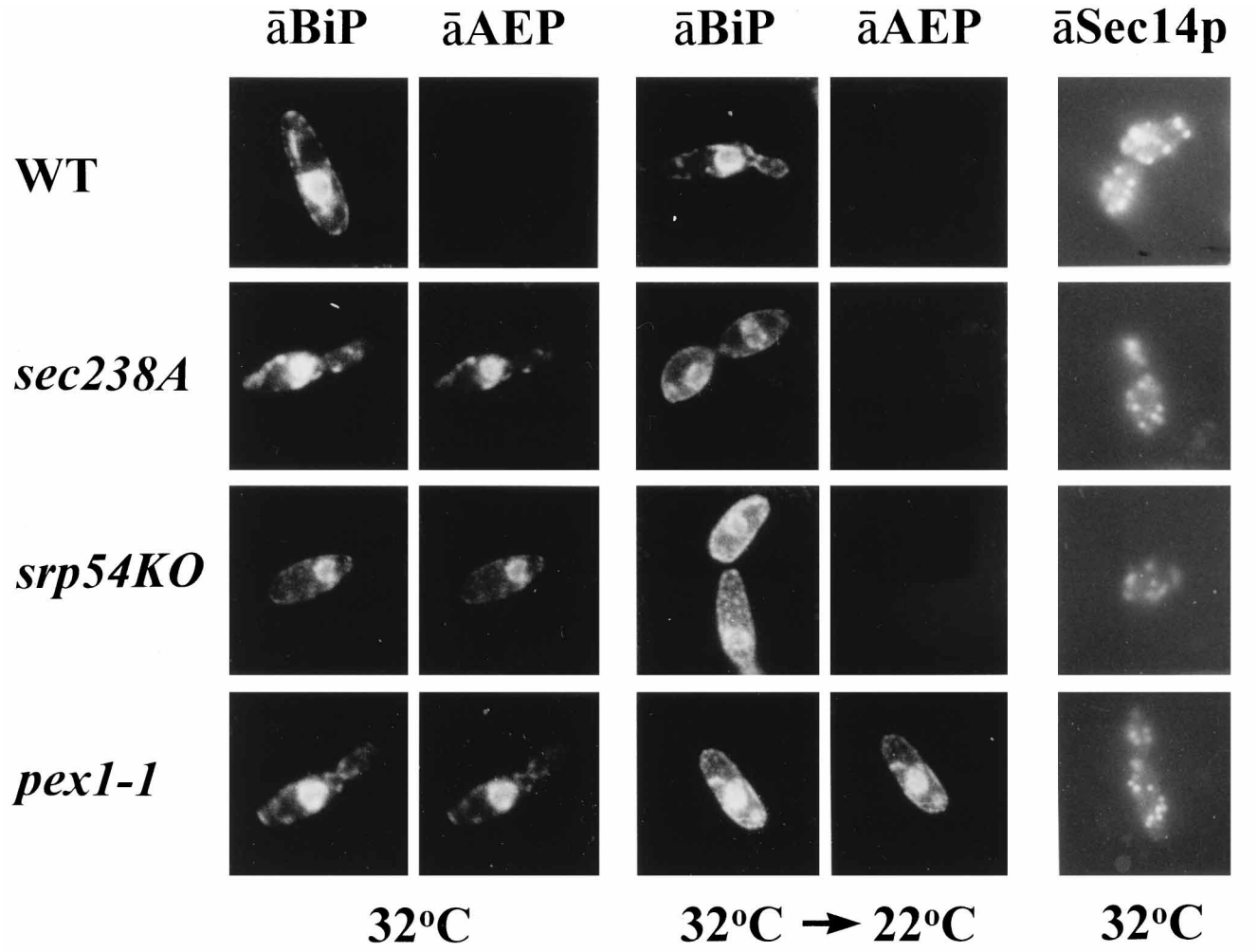

FIG. 7. Intracellular AEP in protein secretion-deficient mutants is localized to the ER. Wild-type and mutant strains were grown in YEPD medium at 32°C until an OD_{600} of 1.0 to 1.2. Cell cultures were separated into two aliquots. One aliquot was shifted to 22°C for 3 h, while the second was maintained at 32°C for 3 h. Both aliquots were subjected to double-labeling indirect immunofluorescence with mouse anti-rat BiP and rabbit anti-*Y. lipolytica* AEP primary antibodies. Cells were also treated with rabbit anti-*Y. lipolytica* Sec14p primary antibodies. Primary antibodies were detected with rhodamine-conjugated donkey anti-mouse immunoglobulin G and fluorescein-conjugated goat anti-rabbit immunoglobulin G secondary antibodies. ā, antibody; WT, wild type.

YEPD medium at 32°C were assayed at two growth phases, exponential (OD_{600}, 1.0 to 1.2; cell titer, 5.5×10^7 to 6.0×10^7 cells/ml) and stationary (OD_{600}, 8.0 to 8.5; cell titer, 5.0×10^8 to 5.5×10^8 cells/ml). During exponential growth, all wild-type and mutant cells were of the yeast form. During stationary growth, more than 95% of the wild-type and *pex1-1* mutant cells underwent the dimorphic transition from the yeast to the mycelial form, while all other protein secretion-deficient mutants failed to undergo this transition (see above).

No differences in the rates and efficiencies of delivery of pulse-labeled plasma membrane (Fig. 13 and 14, top panels) and cell wall-associated (Fig. 15 and 16, top panels) proteins were observed between the wild-type and all protein secretion-deficient strains taken from the exponential (yeast) phase of growth at 32°C. The dimorphic transition of wild-type cells from the yeast to the mycelial form upon entry into stationary phase resulted in changes in the composition and relative abundance of plasma membrane and cell wall-associated proteins. Two plasma membrane proteins of 34 and 43 kDa (Fig. 13 and 14, bottom panels) and four cell wall-associated proteins of 28, 47, 51, and 66 kDa (Fig. 15 and 16, bottom panels) were exported to the plasma membrane or cell envelope only in wild-type cells that underwent the dimorphic transition. These proteins were absent or were present in negligible amounts in the plasma membranes or cell envelopes of wild-type cells taken from the yeast phase (compare top and bottom panels for wild-type cells in Fig. 13 and 14 and in Fig. 15 and 16). Additional observations also point at these plasma membrane and cell wall-associated proteins being specific for the mycelial form of *Y. lipolytica*. First, even wild-type cells were unable to undergo the dimorphic transition when grown at 22°C (see above). Consequently, none of the proteins implicated as being specific for the mycelial phase was found in the plasma membranes or cell envelopes of wild-type cells taken from the stationary phase of growth at 22°C (data not shown). Second, the *sec14KO* mutation not only prevents the dimorphic transition (30) but also affects the delivery of plasma membrane and cell envelope proteins specific for the mycelial form (Fig. 14 and 16, respectively). However, both of these *sec14KO* phenotypes could be seen only in cells grown in YEPD at 32°C, and they could be bypassed when cells were grown in oleic acid-containing medium at 32°C (data not shown).

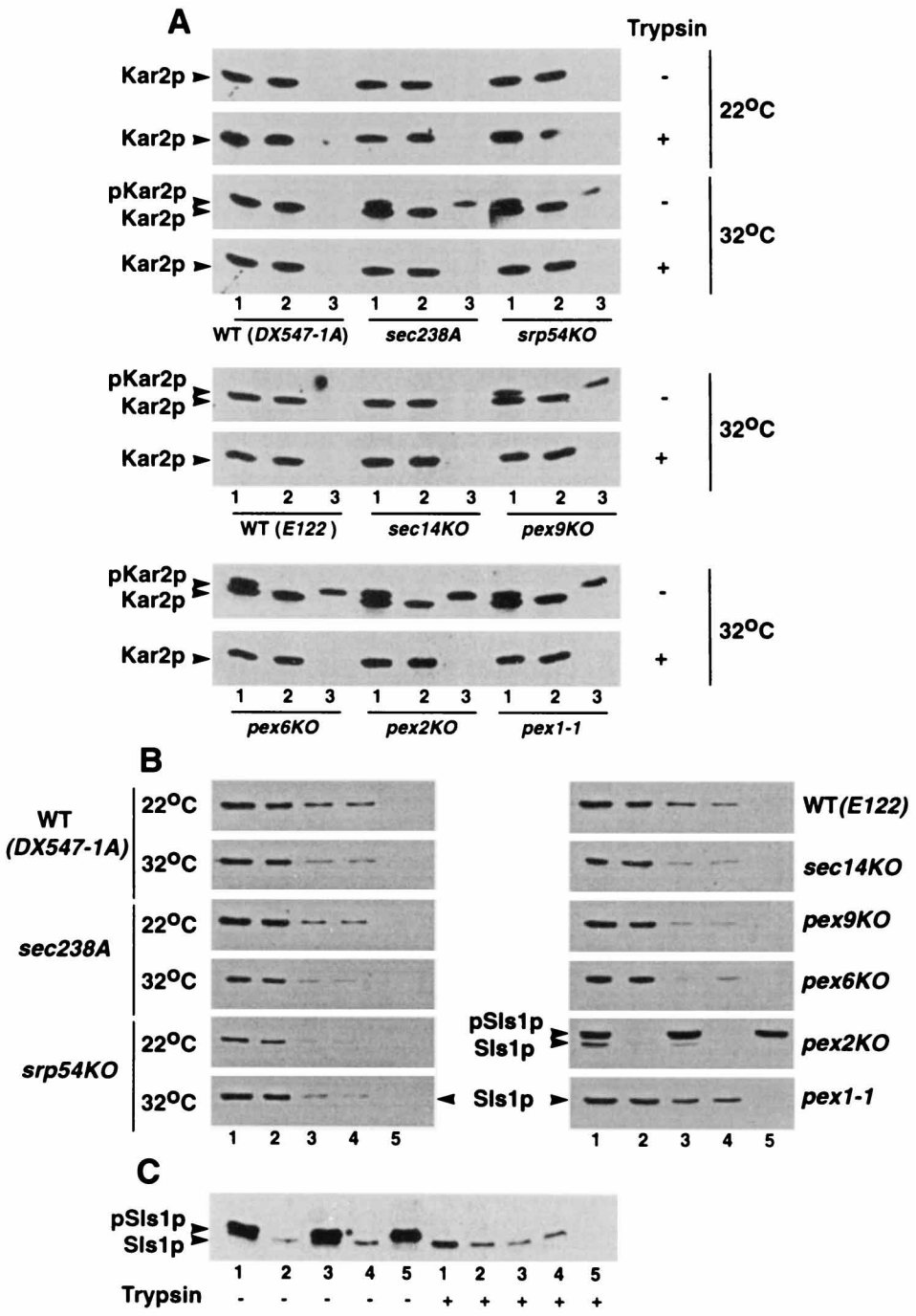

FIG. 8. All protein secretion-deficient mutants are affected in the processing-translocation of pKar2p into the ER, while the *pex2KO* mutant is also affected in the processing-translocation into the ER of pSls1p. Wild-type and mutant strains were grown in YEPD medium at 22 or 32°C and subjected to subcellular fractionation. (A) Equal fractions (0.4% of the total volume) of PNS (lanes 1), 245KgP (lanes 2), and 245KgS (lane 3), either treated with trypsin (10 μg of protease/100 μg of protein) or untreated, were analyzed by immunoblotting with anti-Kar2p antibodies. (B) Equal fractions (0.15% of the total volume) of the PNS (lanes 1), 20KgP (lanes 2), 20KgS (lanes 3), 245KgP (lanes 4), and 245KgS (lanes 5) were analyzed by immunoblotting with anti-Sls1p antibodies. (C) Equal fractions (0.15% of the total volume) of the PNS (lane 1), 20KgP (lane 2), 20KgS (lane 3), 245KgP (lane 4), and 245KgS (lane 5) isolated from *pex2KO* cells grown at 32°C, either treated with trypsin (10 μg of protease/100 μg of protein) or untreated, were analyzed by immunoblotting with anti-Sls1p antibodies. Kar2p, 73-kDa mature form of the Kar2 protein; pKar2p, 75-kDa precursor of Kar2p; Sls1p, the 55-kDa mature form of the Sls1 protein; pSls1p, 58-kDa precursor of Sls1p; WT, wild type.

In pulse-chase experiments, the rates and efficiencies of delivery of plasma membrane and cell envelope proteins specific for the mycelial phase were affected in *sec238A* and *srp54KO* (Fig. 13 and 15, bottom panels) and in *pex9KO*, *pex6KO*, and *pex2KO* (Fig. 14 and 16, bottom panels) mutant strains taken from the stationary phase of growth at 32°C. All of these strains represent protein secretion-deficient mutants that are affected in the dimorphic transition (see above). Similar defects in the delivery of a subset of plasma membrane and cell wall-associated proteins specific for mycelial phase were ob-

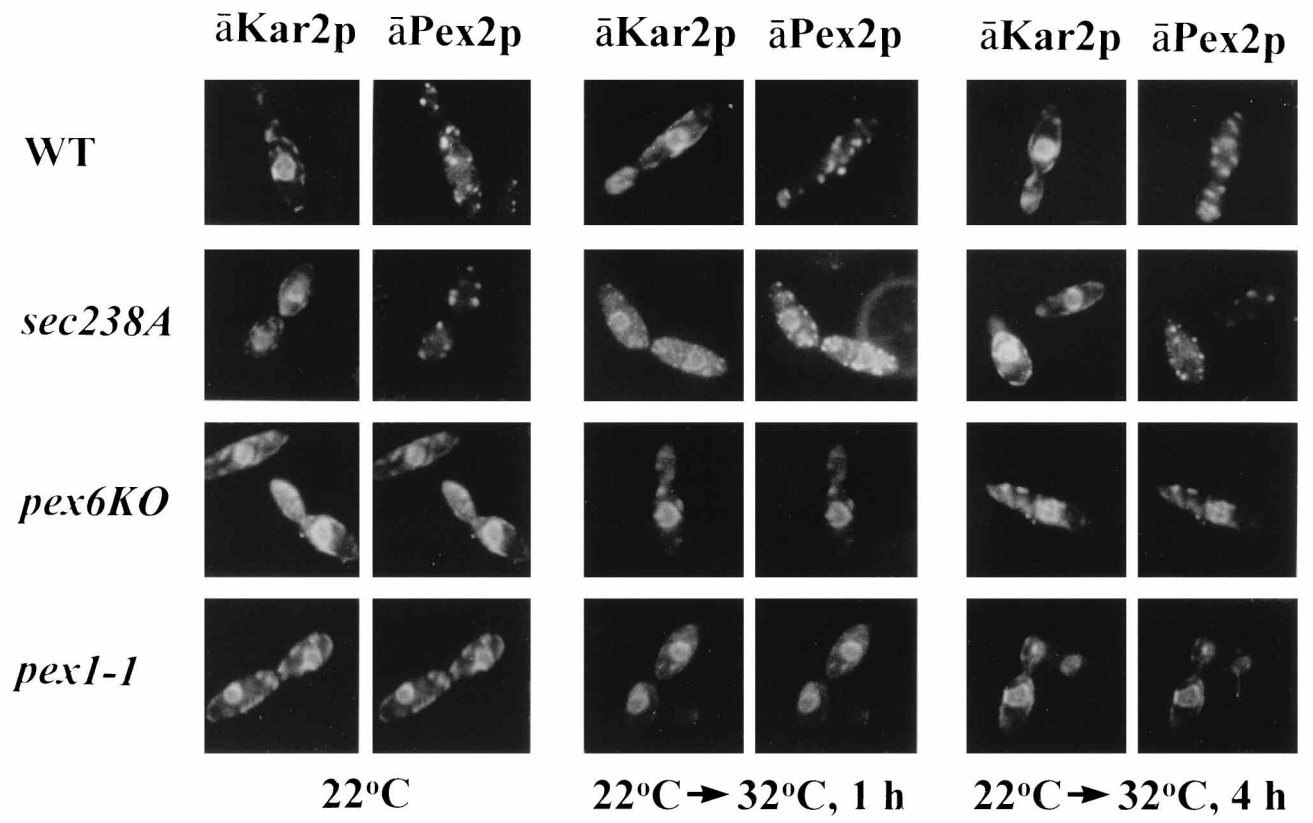

FIG. 9. Pex2p transiently or permanently accumulates in the ER of protein secretion-deficient mutants. Wild-type (WT) and mutant cells were grown in YEPD medium at 22°C until an OD_{600} of 3.5 to 4.0. Cell cultures were separated into three aliquots. Two aliquots were transferred to fresh YEPD medium, and the medium was incubated for 1 or 4 h at 32°C. The third aliquot was processed immediately for microscopical analysis. Cells were processed for double-labeling indirect immunofluorescence with rabbit anti-*Y. lipolytica* Kar2p and guinea pig anti-*Y. lipolytica* Pex2p primary antibodies. Primary antibodies were detected with fluorescein-conjugated goat anti-rabbit immunoglobulin G and rhodamine-conjugated donkey anti-guinea pig immunoglobulin G secondary antibodies. ā, antibody.

served in the *pex5KO*, *pex16KO*, and *pex17KO* mutants (data not shown), which are also unable to undergo the dimorphic transition but which are not deficient in the secretion of proteins into the external medium. In contrast, the rates and efficiencies of export of pulse-labeled proteins specific for the mycelial phase to the plasma membrane (Fig. 14, bottom panel) and the cell envelope (Fig. 16, bottom panel) were unaltered in the protein secretion-deficient mutant *pex1-1* strain, which is able to undergo the dimorphic transition.

It is noteworthy that in wild-type strains, the rate of delivery of plasma membrane and cell wall-associated proteins specific for the mycelial form was significantly lower than the rate of secretion of mAEP and other proteins into the extracellular medium. Mycelial-form-specific proteins appeared in the plasma membrane and cell envelope by 15 min of chase, and their rates of export to the cell surface reached steady state by 60 min of chase (Fig. 13 to 16). In contrast, pulse-labeled mAEP and other secretory proteins appeared in the culture supernatants of wild-type strains at the earliest chase point taken (2 to 2.5 min), and, already by 10 to 20 min of chase, protein secretion into the culture supernatants was almost complete (Fig. 2 and 3).

DISCUSSION

Here, we report the identification and characterization of *Y. lipolytica* mutants blocked in protein secretion. Previous studies have shown that all *S. cerevisiae* mutants specifically blocked in secretion are also defective in cell surface growth. Therefore, *S. cerevisiae* apparently has one major pathway that is common for the secretion of proteins into the cell envelope-external medium and for the export of materials required for plasma membrane and cell wall synthesis (24, 35–37, 47, 60, 62). The present study provides the first evidence that protein secretion and cell surface growth in the yeast *Y. lipolytica* are served by distinct pathways. This study also demonstrates that some peroxins previously identified to be essential for the assembly of functionally intact peroxisomes are also required for protein secretion into the external medium and for the exit of plasma membrane and cell wall-associated proteins specific for the mycelial form of *Y. lipolytica*. We also show that in *Y. lipolytica*, the trafficking of proteins to the external medium and the delivery of some proteins to the peroxisomal membrane occur via the ER and require several components in common. Therefore, the secretory pathway in *Y. lipolytica* can play an essential role in the assembly of functionally intact peroxisomes.

We use the dimorphic yeast *Y. lipolytica* to study the mechanisms involved in coordinating cell surface growth, protein secretion, and peroxisome biogenesis. *Y. lipolytica* is widely divergent from both *S. cerevisiae* and *Schizosaccharomyces pombe* (4, 45). *Y. lipolytica* is a useful experimental organism to investigate cell surface dynamics, because it exists in developmentally distinct yeast and mycelial forms (50). The characteristic dimorphic transition from yeast to mycelium is dependent on both the growth medium composition and phase of growth

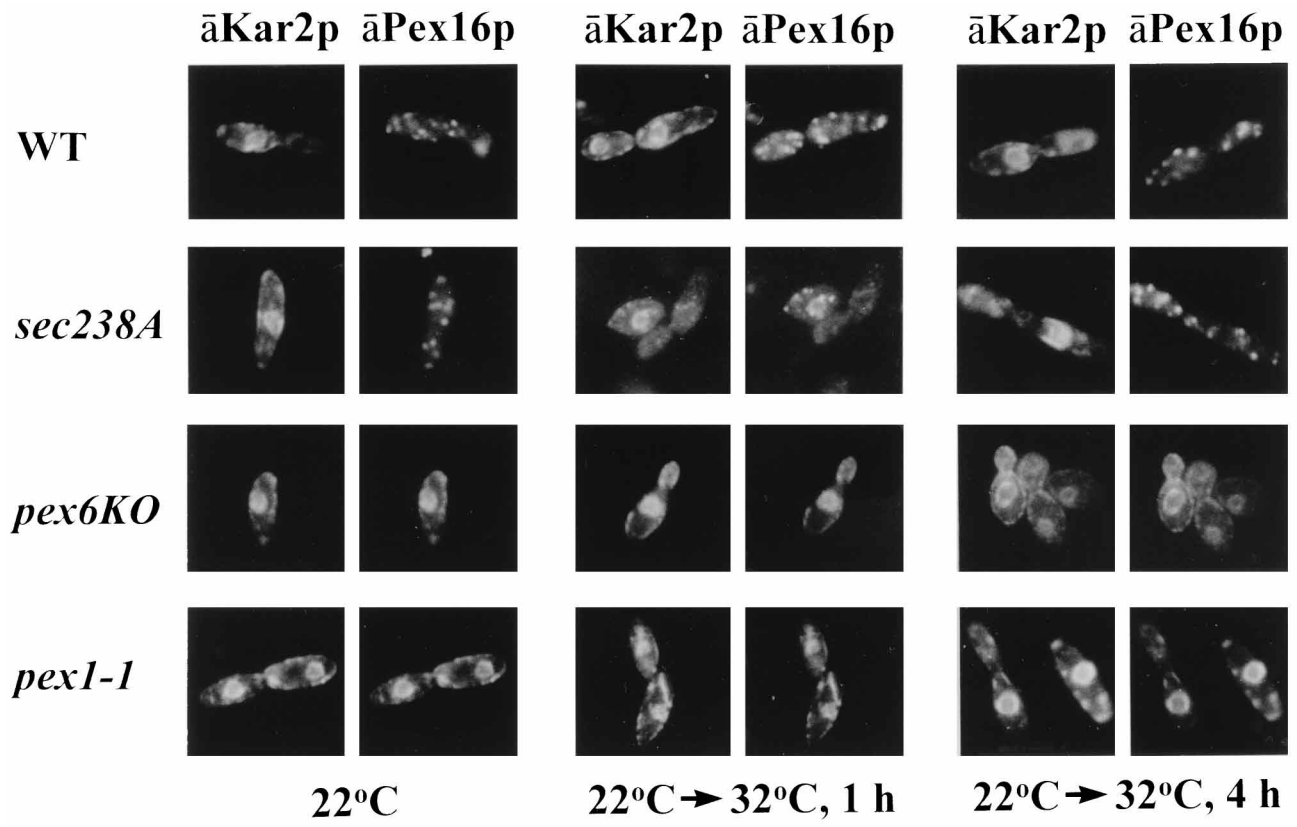

FIG. 10. Pex16p transiently or permanently accumulates in the ER of protein secretion-deficient mutants. Wild-type (WT) and mutant cells were grown and processed for immunofluorescence microscopy with anti (ā)-*Y. lipolytica* Kar2p and guinea pig anti (ā)-*Y. lipolytica* Pex16p primary antibodies as described in the legend to Fig. 9.

and represents a specific developmental program that involves changes in cell morphology (ovoid to filamentous), mode of growth (exponential to linear), and mechanism of cell division (budding to septation) (see references 30 and 50 and this study).

Y. lipolytica has been used extensively to study secretion because of its greater secretory capacity compared to those of *S. cerevisiae* or *S. pombe* and because of its industrial use in protein production. Among yeast species, *Y. lipolytica* is one of the highest producers of extracellular proteins (alkaline, neutral, and acid proteases, APs, and RNase and lipases) and is capable of secreting AEP to levels of 1 to 2 g/liter (40). Moreover, while most secreted proteins of *S. cerevisiae* remain in the cell envelope (23), many proteins secreted by *Y. lipolytica* accumulate outside the cell envelope in the external medium (23, 42). Extensive peroxisome proliferation during growth on oleic acid, combined with the availability of powerful genetic tools, also makes *Y. lipolytica* ideally suited for genetic studies in peroxisome biogenesis (38). Together, these characteristics of *Y. lipolytica* make it a powerful model system for studying the relationships among protein secretion, modes of cell surface growth, and peroxisome biogenesis.

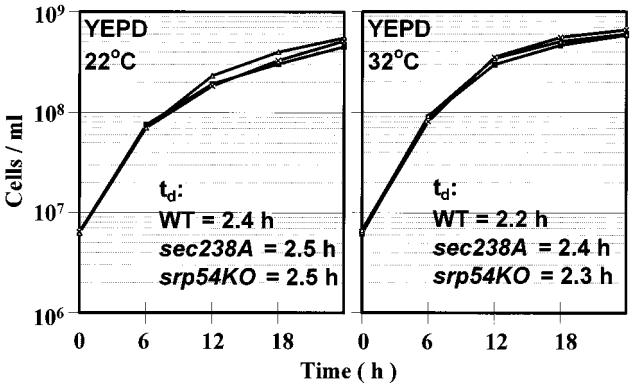

FIG. 11. The *sec238A* and *srp54KO* mutant strains are unaffected in growth in YEPD medium even at the temperature at which protein secretion is impaired. Growth curves and doubling times (t_d) of the wild-type (WT) *DX547-1A* (■) and the mutant *sec238A* (x) and *srp54KO* (△) strains grown in YEPD at 22 or 32°C are shown.

The results of genetic and biochemical analyses of *Y. lipolytica* mutants affected in protein secretion are summarized in the model depicted in Fig. 17. This model predicts the existence of four distinct secretory pathways that serve protein secretion, cell surface enlargement during yeast and mycelial modes of growth, and peroxisome biogenesis. All six protein secretion-deficient mutants reported here were affected in the delivery of AEP to the extracellular medium and accumulated pAEP in the ER. The rates and efficiencies of secretion of all other secretory proteins were affected in these mutants to a similar extent. These data suggest that in *Y. lipolytica*, Sec238p, Srp54p, Pex1p, Pex2p, Pex6p, and Pex9p are essential for the exit from the ER of proteins destined to be secreted. The proteins encoded by the genes *PEX1* and *PEX6*, which are required for the exit of pAEP from the ER, are also essential

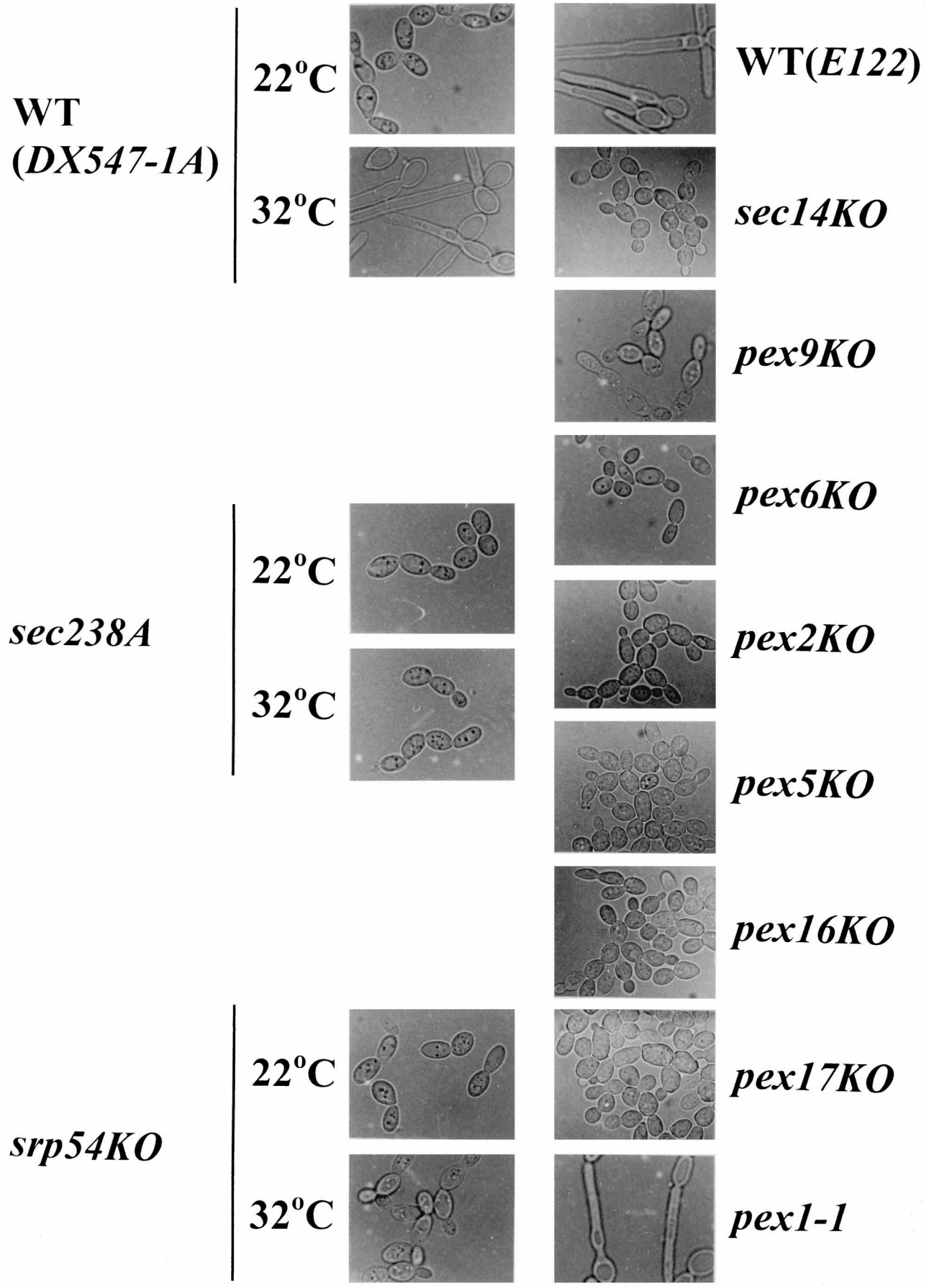
WT
(DX547-1A)
22°C
32°C
WT(E122)
sec14KO
pex9KO
pex6KO
sec238A
22°C
32°C
pex2KO
pex5KO
pex16KO
srp54KO
22°C
32°C
pex17KO
pex1-1

FIG. 12. Some but not all protein secretion mutants are affected in the dimorphic transition from the yeast to the mycelial form. Wild-type (WT) and mutant strains were grown in YEPD medium at 22 or 32°C until the late stationary phase of growth (OD_{600} of 11.0 to 12.0; cell titer, ~6.0×10^8 to 6.6×10^8 cells/ml). Cell morphology after 24 h of growth is shown.

for the exit of two peroxisomal membrane proteins, Pex2p and Pex16p, from the ER. Both Pex1p (59) and Pex6p (39) are members of the AAA protein family of *N*-ethylmaleimide-sensitive fusion protein (NSF)-like ATPases, which are essential not only for peroxisome biogenesis (25) but also for homo- and heterotypic fusion events required for the assembly of other organelles (12). Furthermore, temperature-sensitive mutations in two other proteins, Sec238p and Srp54p, which are essential for the exit of pAEP from the ER caused a delay in the exit of Pex2p and Pex16p from the ER at the restrictive temperature. These data indicate that the delivery of proteins to the extracellular medium and the trafficking of some proteins to the peroxisomal membrane occur via the ER and require the activities of several components in common. Therefore, in *Y. lipolytica*, the secretory pathway can play an essential role in peroxisome biogenesis. A role for the ER in the trafficking of membrane proteins to peroxisomes in mammalian and yeast cells has also been suggested by some recent observations (2, 7, 17, 60).

It should be noted that not all components essential for the exit of secretory proteins from the ER are required for the trafficking of Pex2p and Pex16p via the ER. While the exit of pAEP from the ER was prevented by the *pex2KO* and *pex9KO* mutations, the trafficking of Pex2p and Pex16p via the ER was unaffected by these mutations. Furthermore, while mutations in the *SEC238* and *SRP54* genes abolished the trafficking of pAEP via the ER at the restrictive temperature, both mutations caused a delay in, but did not prevent, the exit of Pex2p and Pex16p from the ER. Sec238p and Srp54p may represent dispensable components of the machinery involved in the trafficking of some peroxisomal membrane proteins via the ER and, possibly, can be substituted, at least in part, by Pex1p and/or Pex6p. Taken together, these data suggest that secretory routes that function in protein secretion and the delivery of some proteins to the peroxisomal membrane not only have several common steps but also have distinct steps. Thus, these two secretory routes can diverge at the level of the ER.

Despite Pex2p and Pex9p not being required and Sec238p and Srp54p being redundant for the exit of some peroxisomal membrane proteins from the ER, all of these components are essential for the assembly of functionally intact peroxisomes. What roles these proteins might play in peroxisome biogenesis is currently being investigated.

Five of the six components involved in the exit of secretory proteins from the ER are also required for the export of a subset of plasma membrane and cell wall-associated proteins specific for the mycelial form of *Y. lipolytica*. The *sec238A*, *srp54KO*, *pex2KO*, *pex6KO*, and *pex9KO* mutants affected in these components are deficient in the dimorphic transition from the yeast to the mycelial form. Based on this observation, we speculate that similarly to the export of proteins into the extracellular medium, the delivery of mycelial-form-specific proteins to the plasma membrane and to the cell envelope may occur via the ER and that both of these routes of protein traffic require several components in common. On the other hand, not all components essential for the exit of secretory proteins from the ER are also required for the delivery of plasma membrane and cell wall-associated proteins specific for the mycelial form of *Y. lipolytica* (and vice versa). The *pex1-1* mutation affected the exit of secretory proteins from the ER but did not impair the export of mycelial-form-specific proteins to the plasma membrane and cell envelope. In contrast, mutations in the *SEC14*, *PEX5*, *PEX16*, and *PEX17* genes abolished the delivery of plasma membrane and cell wall-associated proteins specific for the mycelial form but did not prevent the exit of secretory proteins from the ER and their export to the extracellular medium. Furthermore, in the wild-type strains, the rates of secretion of mAEP and other proteins into the extracellular medium significantly exceed the rates of delivery of plasma membrane and cell wall-associated proteins specific for the mycelial form. These data suggest that secretory routes that are involved in protein export to the extracellular medium and in the delivery of mycelial-form-specific proteins to the plasma membrane and cell envelope have several distinct steps which may proceed with different rates.

The exit of the peroxisomal membrane proteins Pex2p and Pex16p from the ER and the export of mycelial-form-specific proteins to the plasma membrane and cell envelope share at least one step but also have at least one distinct step. The *pex6KO* mutation affected both of these protein trafficking routes, while mutation of the *PEX1* gene prevented the exit of Pex2p and Pex16p from the ER but did not affect the export of plasma membrane and cell wall-associated proteins specific for the mycelial form. Moreover, while the *sec238A* and *srp54KO* mutations at the restrictive temperature delayed, but did not prevent, the trafficking of Pex2p and Pex16p from the ER, both mutations did abolish the delivery of mycelial-phase-specific proteins to the cell surface.

Another important aspect of this study is the demonstration of a functional relationship between peroxisome biogenesis and a specific process in cell morphogenesis, i.e., the dimorphic transition from the yeast to the mycelial form of *Y. lipolytica*. Most of the components essential for peroxisome biogenesis are also required for the dimorphic transition and for the delivery of mycelial-form-specific proteins to the plasma membrane and cell envelope. These components include Pex6p, which is required for the exit of the peroxisomal membrane proteins Pex2p and Pex16p from the ER; Sec238p and Srp54p, which are redundant for the exit of peroxisomal membrane proteins from the ER (see above) but which perform an essential role in peroxisome biogenesis downstream of that process; and Pex2p, Pex5p, Pex9p, Pex16p, and Pex17p, which are involved in the assembly of functionally intact peroxisomes but which are not required for the exit of the peroxisomal membrane proteins Pex2p and Pex16p from the ER. The essential role of peroxisomes in the export of proteins for plasma membrane and cell wall synthesis during mycelial growth demonstrates a novel function for this organelle. This function is essential even in glucose-containing medium, i.e., under conditions not requiring intact peroxisomes for the utilization of a carbon source. It should be noted that the functional coordination between peroxisome biogenesis and a specific stage of sexual development has recently been demonstrated for the filamentous fungus *Podospora anserina*. The peroxisome-associated protein Car1p (a structural homolog of *Y. lipolytica* Pex2p) is essential for karyogamy (6).

None of the mutations affecting protein secretion, peroxisome biogenesis, and/or the dimorphic transition had any effect on the export of proteins to the plasma membrane and cell envelope during the yeast phase of growth. Therefore, cell

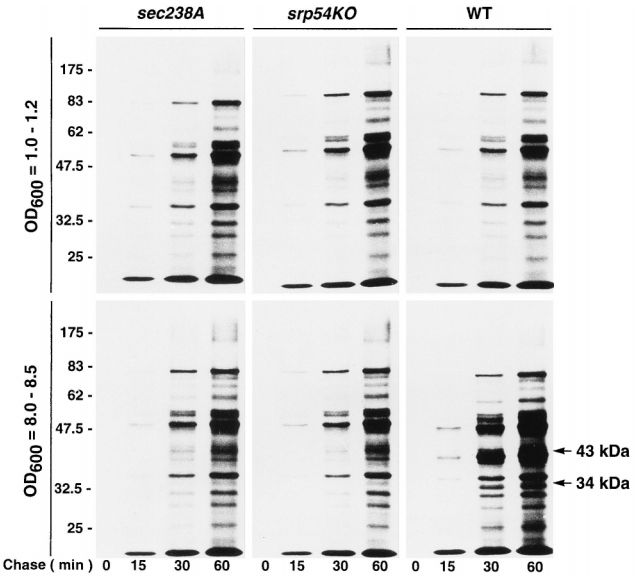

FIG. 13. The *sec238A* and *srp54KO* mutations do not affect the rate of protein transit to plasma membrane during the yeast phase of growth but do impair the efficiency of delivery of some plasma membrane proteins specific for the mycelial form of *Y. lipolytica*. Wild-type (WT) and mutant cells were grown in YEPD medium at 32°C until an OD_{600} of 1.0 to 1.2 or an OD_{600} of 8.0 to 8.5, pulse-labeled at 32°C for 1.5 min with L-[^{35}S]methionine, and subjected to chase with unlabeled methionine. Samples were taken at the indicated times postchase, and plasma membranes were isolated and analyzed by SDS-PAGE and fluorography. Numbers at left indicate the migration of molecular mass standards (in kilodaltons). The positions of 34- and 43-kDa proteins specific for the mycelial form of *Y. lipolytica* are indicated by arrows.

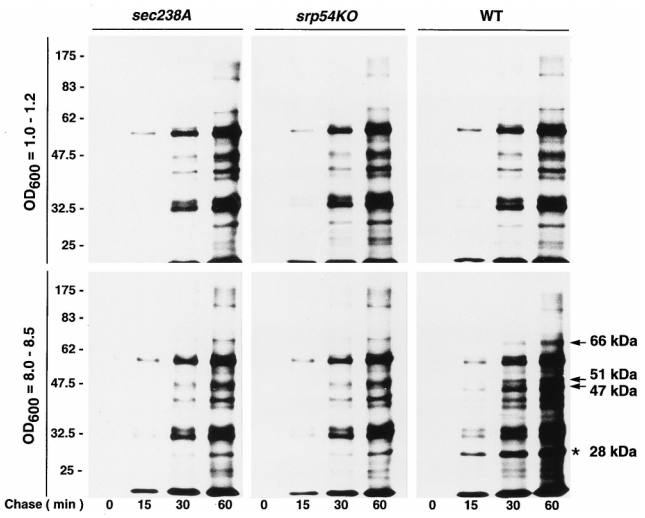

FIG. 15. The *sec238A* and *srp54KO* mutations do not compromise the transport of proteins to the cell envelope during the yeast phase of growth but do affect the efficiency of delivery of some cell wall-associated proteins specific for the mycelial form of *Y. lipolytica*. Wild-type (WT) and mutant cells were grown in YEPD medium at 32°C until an OD_{600} of 1.0 to 1.2 or an OD_{600} of 8.0 to 8.5, pulse-labeled at 32°C for 1.5 min with L-[^{35}S]methionine, and subjected to chase with unlabeled methionine. Samples were taken at the indicated times postchase, and cell wall-associated proteins were extracted with high pH and were analyzed by SDS-PAGE and fluorography. Numbers at left indicate the migration of molecular mass standards (in kilodaltons). The positions of 47-, 51-, and 66-kDa proteins specific for the mycelial form of *Y. lipolytica* are indicated by arrows. The position of a 28-kDa protein highly induced during mycelial growth of the wild-type strain is indicated by asterisk.

surface growth of *Y. lipolytica* cells in the yeast developmental form can be served by a secretory pathway that is distinct from the other three secretory routes. It remains unclear whether protein trafficking through this distinct secretory pathway occurs via the ER or whether some proteins at least could be transported via a nonclassical secretory route. The existence of at least two nonclassical secretory pathways that are not mediated by ER-derived vesicles has recently been demonstrated for *S. cerevisiae* (9, 10, 33).

It should be noted that mutations in the *SEC238*, *SRP54*, *PEX1*, *PEX2*, *PEX6*, and *PEX9* genes not only affected the exit of pAEP and, in the case of the *pex1* and *pex6* mutations, of Pex2p and Pex16p from the ER but that they also compromised the translocation of Kar2p and, in the case of the *pex2KO* mutation, of Sls1p into the ER lumen and caused a decrease in the buoyant density of ER elements. Although substantial amounts of pKar2p accumulated in the cytosol of secretory mutants grown at the temperatures restrictive for secretion, no significant differences in the levels of the mature, ER-associated form of Kar2p were found between the wild-type and mutant strains. These data suggest that the levels of the mature form of Kar2p in the ER lumen cannot be limiting for protein translocation into, or protein exit from, the ER in

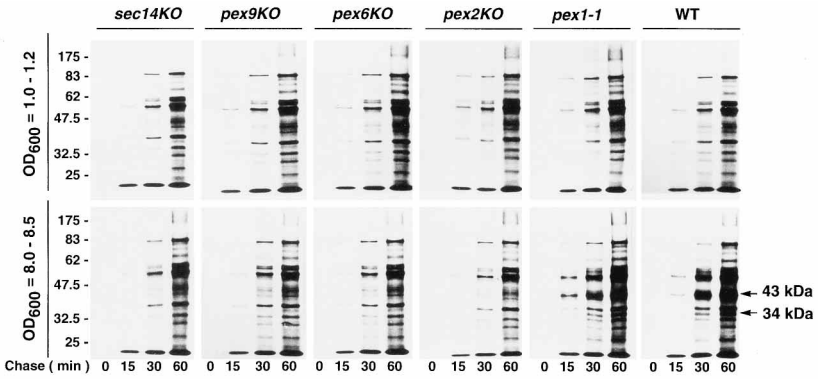

FIG. 14. Effects of the *sec14KO*, *pex9KO*, *pex6KO*, *pex2KO*, and *pex1-1* mutations on the efficiency of delivery of proteins to the plasma membrane. Cells of the wild-type (WT) and mutant strains were grown in YEPD medium at 32°C until an OD_{600} of 1.0 to 1.2 or an OD_{600} of 8.0 to 8.5, pulse-labeled at 32°C for 1.5 min with L-[^{35}S]methionine, and subjected to chase with unlabeled methionine. Samples were taken at the indicated times postchase, and plasma membranes were isolated and analyzed by SDS-PAGE and fluorography. Numbers at left indicate the migration of molecular mass standards (in kilodaltons). The positions of 34- and 43-kDa proteins specific for the mycelial form of *Y. lipolytica* are indicated by arrows.

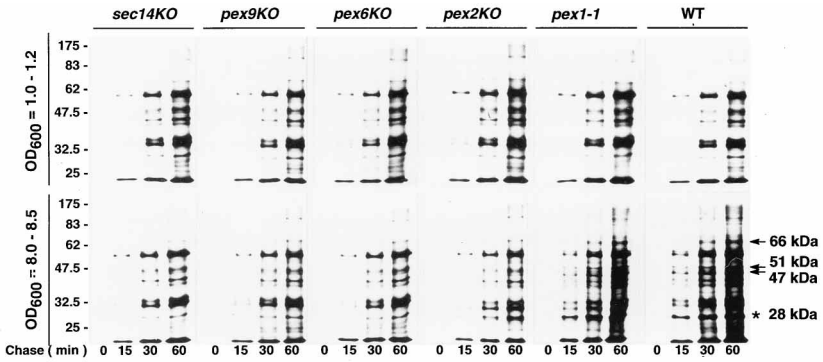

FIG. 16. Effects of the *sec14KO*, *pex9KO*, *pex6KO*, *pex2KO*, and *pex1-1* mutations on the efficiency of delivery of proteins to the cell envelope. Cells of the wild-type (WT) and mutant strains were grown in YEPD medium at 32°C, pulse-labeled with L-[^{35}S]methionine, and subjected to chase as described in the legend to Fig. 15. Samples were taken at the indicated times postchase, and cell wall-associated proteins were extracted by high pH and analyzed by SDS-PAGE and fluorography. Numbers at left indicate the migration of molecular mass standards (in kilodaltons). The positions of proteins specific for the mycelial form of *Y. lipolytica* or highly induced during the transition from yeast to mycelial growth are indicated as described for Fig. 15.

these protein secretion-deficient mutants. The mechanism(s) by which these mutations affect the translocation of some proteins into the ER and alter the density of ER elements requires further analysis. Various mutational blocks in the exit of secretory and peroxisomal membrane proteins from the ER lead to the accumulation of proteins, normally secreted by wild-type cells, within the ER lumen. We speculate that such an accumulation of cargo proteins that are unable to exit the ER can, in turn, cause changes in the suborganellar localization and/or conformation of components essential for protein translocation into the ER lumen, thereby affecting protein translocation.

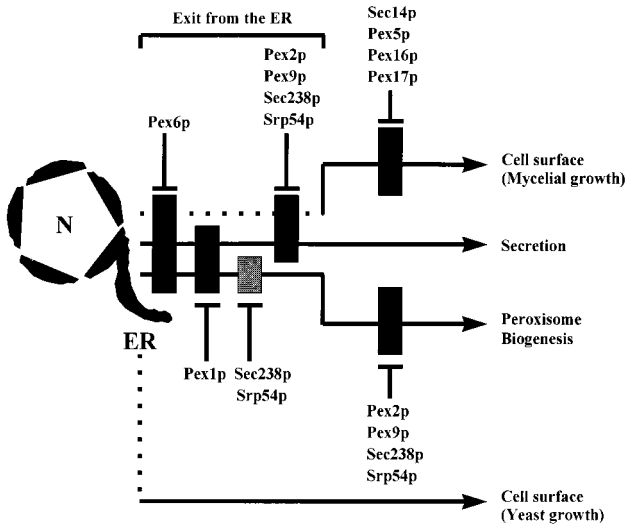

FIG. 17. Model of the secretory pathways serving protein secretion, cell surface enlargement during yeast and mycelial growth, and peroxisome biogenesis in *Y. lipolytica*. In this model, two routes serving the exit of secretory proteins and of peroxisomal membrane proteins from the ER overlap but also have distinct steps and, therefore, diverge at the level of the ER. Branching of a third secretory route functioning in the delivery of mycelial-phase-specific proteins to the plasma membrane and cell envelope at the level of the ER (dotted line) can be suggested from the present data, although this has not been demonstrated directly. Export of proteins for plasma membrane and cell wall synthesis during the yeast mode of growth is mediated by a fourth secretory pathway, although it remains unclear whether or not protein trafficking through this pathway occurs via the ER (dotted line). Protein products of the *SEC238*, *SRP54*, *SEC14*, *PEX1*, *PEX2*, *PEX5*, *PEX6*, *PEX9*, *PEX16*, and *PEX17* genes perform essential roles at various steps of the different secretory pathways and are required for the exit of proteins at, or downstream of, the ER (for a detailed description, see the text). The gray box indicates that the *sec238A* and *srp54KO* mutations result in delay, but not blocking, of the exit of the peroxisomal membrane proteins Pex2p and Pex16p from the ER. Therefore, Sec238p and Srp54p may be dispensable for this process. N, nucleus.

The results described herein provide evidence for the existence of four distinct secretory pathways that serve (i) protein secretion, (ii) export of proteins for plasma membrane and cell wall synthesis during the yeast mode of growth, (iii) delivery of proteins for plasma membrane and cell wall synthesis during the mycelial mode of growth, and (iv) peroxisome biogenesis in *Y. lipolytica*. At least two of these secretory pathways functioning in protein secretion into the extracellular medium and delivery of proteins for the assembly of peroxisomal membrane diverge at the level of the ER. The mechanisms by which these secretory pathways function are currently being investigated.

ACKNOWLEDGMENTS

This work was supported by a grant from the Medical Research Council (MRC) of Canada to R.A.R. R.A.R. is an MRC Scientist and an International Research Scholar of the Howard Hughes Medical Institute.

REFERENCES

1. **Abeijon, C., P. Orlean, P. W. Robins, and C. B. Hirschberg.** 1989. Topography of glycosylation in yeast: characterization of GDP-mannose transport and lumenal guanosine diphosphatase activities in Golgi-like vesicles. Proc. Natl. Acad. Sci. USA **86:**6935–6939.
2. **Baerends, R. J. S., S. W. Rasmussen, R. E. Hilbrands, M. van der Heide, K. N. Faber, P. T. W. Reuvekamp, J. A. K. W. Kiel, J. M. Cregg, I. J. van der Klei, and M. Veenhuis.** 1996. The *Hansenula polymorpha PER9* gene encodes a peroxisomal membrane protein essential for peroxisome assembly and integrity. J. Biol. Chem. **271:**8887–8894.
3. **Barlowe, C., L. Orci, T. Yeung, M. Hosobuchi, S. Hamamoto, N. Salama, M. F. Rexach, M. Ravazzola, M. Amherdt, and R. Schekman.** 1994. COPII: a membrane coat formed by Sec proteins that drive vesicle budding from the endoplasmic reticulum. Cell **77:**895–907.
4. **Barns, S. M., D. J. Lane, M. L. Sogin, C. Bibeau, and W. G. Weisburg.** 1991. Evolutionary relationships among pathogenic *Candida* species and relatives. J. Bacteriol. **173:**2250–2255.
5. **Bednarek, S. Y., M. Ravazzola, M. Hosobuchi, M. Amherdt, A. Perrelet, R. Schekman, and L. Orci.** 1995. COPI- and COPII-coated vesicles bud directly from the endoplasmic reticulum in yeast. Cell **83:**1183–1196.
6. **Berteaux-Lecellier, V., M. Picard, C. Thompson-Coffe, D. Zickler, A. Panvier-Adoutte, and J.-M. Simonet.** 1995. A nonmammalian homolog of the *PAF1* gene (Zellweger syndrome) discovered as a gene involved in caryogamy in the fungus Podospora anserina. Cell **81:**1043–1051.
7. **Bodnar, A. G., and R. A. Rachubinski.** 1991. Characterization of the integral membrane polypeptides of rat liver peroxisomes isolated from untreated and clofibrate-treated rats. Biochem. Cell Biol. **69:**499–508.
8. **Boisramé, A., J.-M. Beckerich, and C. Gaillardin.** 1996. Sls1p, an endoplas-

mic reticulum component, is involved in the protein translocation process in the yeast *Yarrowia lipolytica*. J. Biol. Chem. **271:**11668–11675.
9. **Cleves, A. E., D. N. W. Cooper, S. H. Barondes, and R. B. Kelly.** 1996. A new pathway for protein export in *Saccharomyces cerevisiae*. J. Cell Biol. **133:** 1017–1026.
10. **Cleves, A. E., and R. B. Kelly.** 1996. Protein translocation: rehearing the ABCs. Curr. Biol. **6:**276–278.
11. **Coligan, J. E., B. M. Dunn, H. L. Ploegh, D. W. Speicher, and P. T. Wingfield (ed.).** 1995. Current protocols in protein science. John Wiley & Sons, New York, N.Y.
12. **Denesvre, C., and V. Malhotra.** 1996. Membrane fusion in organelle biogenesis. Curr. Opin. Cell Biol. **8:**519–523.
13. **Distel, B., R. Erdmann, S. J. Gould, G. Blobel, D. I. Crane, J. M. Cregg, G. Dodt, Y. Fujiki, J. M. Goodman, W. W. Just, J. A. K. W. Kiel, W.-H. Kunau, P. B. Lazarow, G. P. Mannaerts, H. Moser, T. Osumi, R. A. Rachubinski, A. Roscher, S. Subramani, H. F. Tabak, D. Valle, I. van der Klei, P. P. van Veldhoven, and M. Veenhuis.** 1996. A unified nomenclature for peroxisome biogenesis. J. Cell Biol. **135:**1–3.
14. **Eitzen, G. A., J. D. Aitchison, R. K. Szilard, M. Veenhuis, W. M. Nuttley, and R. A. Rachubinski.** 1995. The *Yarrowia lipolytica* gene *PAY2* encodes a 42-kDa peroxisomal integral membrane protein essential for matrix protein import and peroxisome enlargement but not for peroxisome membrane proliferation. J. Biol. Chem. **270:**1429–1436.
15. **Eitzen, G. A., R. K. Szilard, and R. A. Rachubinski.** Enlarged peroxisomes are present in oleic acid-grown *Yarrowia lipolytica* overexpressing the *PEX16* gene encoding an intraperoxisomal peripheral membrane peroxin. J. Cell Biol., in press.
16. **Eitzen, G. A., V. I. Titorenko, J. J. Smith, M. Veenhuis, R. K. Szilard, and R. A. Rachubinski.** 1996. The *Yarrowia lipolytica* gene *PAY5* encodes a peroxisomal integral membrane protein homologous to the mammalian peroxisome assembly factor PAF-1. J. Biol. Chem. **271:**20300–20306.
17. **Elgersma, Y.** 1995. Transport of proteins and metabolites across the peroxisomal membrane in *Saccharomyces cerevisiae*. Ph.D. thesis. University of Amsterdam, Amsterdam, The Netherlands.
18. **Fabre, E., C. Tharaud, and C. Gaillardin.** 1992. Intracellular transit of a yeast protease is rescued by trans-complementation with its prodomain. J. Biol. Chem. **267:**15049–15055.
19. **Franzusoff, A., J. Rothblatt, and R. Schekman.** 1991. Analysis of polypeptide transit through yeast secretory pathway. Methods Enzymol. **194:**662–674.
20. **Goodman, J. M., S. B. Trapp, H. Hwang, and M. Veenhuis.** 1990. Peroxisomes induced in *Candida boidinii* by methanol, oleic acid and D-alanine vary in metabolic function but share common integral membrane proteins. J. Cell Sci. **97:**193–204.
21. **Gumbiner, B., and R. B. Kelly.** 1982. Two distinct intracellular pathways transport secretory and membrane glycoproteins to the surface of pituitary tumor cells. Cell **28:**51–59.
22. **Harsay, E., and A. Bretscher.** 1995. Parallel secretory pathways to the cell surface in yeast. J. Cell Biol. **131:**297–310.
23. **Heslot, H., and C. Gaillardin.** 1992. Molecular biology and genetic engineering of yeast. CRC Press, Boca Raton, Fla.
24. **Kaiser, C. A., and R. Schekman.** 1990. Distinct sets of *SEC* genes govern transport vesicle formation and fusion early in the secretory pathway. Cell **61:**723–733.
25. **Kunau, W.-H., A. Beyer, T. Franken, K. Götte, M. Marzioch, J. Saidowsky, A. Skaletz-Rorowski, and F. F. Wiebel.** 1993. Two complementary approaches to study peroxisome biogenesis in *Saccharomyces cerevisiae*: forward and reversed genetics. Biochimie **75:**209–224.
26. **Kyhse-Andersen, J.** 1984. Electroblotting of multiple gels: a simple apparatus without buffer tank for rapid transfer of proteins from polyacrylamide to nitrocellulose. J. Biochem. Biophys. Methods **10:**203–209.
27. **Laemmli, U. K.** 1970. Cleavage of structural proteins during the assembly of the head of bacteriophage T4. Nature (London) **227:**680–685.
28. **Lanzetta, P. A., L. J. Alvarez, P. S. Reinach, and O. A. Candia.** 1979. An improved assay for nanomole amounts of inorganic phosphate. Anal. Biochem. **100:**95–97.
29. **Lee, I. H., and D. M. Ogrydziak.** *Yarrowia lipolytica SRP54* homolog and translocation of Kar2p. Yeast, in press.
30. **Lopez, M. C., J.-M. Nicaud, H. B. Skinner, C. Vergnolle, J. C. Kader, V. A. Bankaitis, and C. Gaillardin.** 1994. A phosphatidylinositol/phosphatidylcholine transfer protein is required for differentiation of the dimorphic yeast *Yarrowia lipolytica* from the yeast to the mycelial form. J. Cell Biol. **125:**113–127.
31. **Matoba, S., J. Fukayama, R. A. Wing, and D. M. Ogrydziak.** 1988. Intracellular precursors and secretion of alkaline extracellular protease of *Yarrowia lipolytica*. Mol. Cell. Biol. **8:**4904–4916.
32. **Mellman, I., and K. Simons.** 1992. The Golgi complex: in vitro veritas? Cell **68:**829–840.
33. **Michaelis, S.** 1993. *STE6*, the yeast a-factor transporter. Semin. Cell Biol. **4:**17–27.
34. **Mostov, K., G. Apodaca, B. Aroeti, and C. Okamoto.** 1992. Plasma membrane protein sorting in polarized epithelial cells. J. Cell Biol. **116:**577–583.
35. **Novick, P., C. Field, and R. Schekman.** 1980. Identification of 23 complementation groups required for post-translational events in the yeast secretory pathway. Cell **21:**205–215.
36. **Novick, P., and R. Schekman.** 1979. Secretion and cell-surface growth are blocked in a temperature-sensitive mutant of *Saccharomyces cerevisiae*. Proc. Natl. Acad. Sci. USA **76:**1858–1862.
37. **Novick, P., and R. Schekman.** 1983. Export of major cell surface proteins is blocked in yeast secretory mutants. J. Cell Biol. **96:**541–547.
38. **Nuttley, W. M., A. M. Brade, C. Gaillardin, G. A. Eitzen, J. R. Glover, J. D. Aitchison, and R. A. Rachubinski.** 1993. Rapid identification and characterization of peroxisomal assembly mutants in *Yarrowia lipolytica*. Yeast **9:**507–517.
39. **Nuttley, W. M., A. M. Brade, G. A. Eitzen, M. Veenhuis, J. D. Aitchison, R. K. Szilard, J. R. Glover, and R. A. Rachubinski.** 1994. PAY4, a gene required for peroxisome assembly in the yeast *Yarrowia lipolytica*, encodes a novel member of a family of putative ATPases. J. Biol. Chem. **269:**556–566.
40. **Ogrydziak, D. M.** 1988. Production of alkaline extracellular protease by *Yarrowia lipolytica* Crit. Rev. Biochem. **8:**4904–4916.
41. **Ogrydziak, D. M., S.-C. Cheng, and S. J. Scharf.** 1982. Characterization of *Saccharomycopsis lipolytica* mutants producing lowered levels of alkaline extracellular protease. J. Gen. Microbiol. **128:**2271–2280.
42. **Ogrydziak, D. M., and R. K. Mortimer.** 1977. Genetics of extracellular protease production in *Saccharomycopsis lipolytica*. Genetics **87:**621–632.
43. **Palade, G.** 1975. Intracellular aspects of the process of protein synthesis. Science **189:**347–358.
44. **Pelham, H. R. B.** 1994. About turn for the COPs? Cell **79:**1125–1127.
45. **Pesole, G., M. Lotti, L. Alberghina, and C. Saccone.** 1995. Evolutionary origin of nonuniversal CUGSer codon in some *Candida* species is inferred from a molecular phylogeny. Genetics **141:**903–907.
46. **Pidoux, A. L., and J. Armstrong.** 1992. Analysis of the BiP gene and identification of an ER retention signal in *Schizosaccharomyces pombe*. EMBO J. **11:**1583–1591.
47. **Pryer, N. K., L. J. Wuestehube, and R. Schekman.** 1992. Vesicle-mediated protein sorting. Annu. Rev. Biochem. **61:**471–516.
48. **Rindler, M. J., I. E. Ivanov, H. Plesken, E. Rodriguez-Boulan, and D. D. Sabatini.** 1984. Viral glycoproteins destined for apical or basolateral plasma membrane domains traverse the same Golgi apparatus during their intracellular transport in doubly infected Madin-Darby canine kidney cells. J. Cell Biol. **98:**1304–1319.
49. **Roberts, C. J., C. K. Raymond, C. T. Yamashiro, and T. H. Stevens.** 1991. Methods for studying the yeast vacuole. Methods Enzymol. **194:**644–661.
50. **Rodriguez, C., and A. Dominguez.** 1984. The growth characteristics of *Saccharomycopsis lipolytica*: morphology and induction of mycelium formation. Can. J. Microbiol. **30:**605–612.
51. **Rose, M. D., L. M. Misra, and J. P. Vogel.** 1989. *KAR2*, a karyogamy gene, is the yeast homolog of the mammalian BiP/GRP78 gene. Cell **57:**1211–1221.
52. **Rothman, J. E.** 1994. Mechanisms of intracellular protein transport. Nature (London) **372:**55–63.
53. **Rothman, J. E., and L. Orci.** 1992. Molecular dissection of the secretory pathway. Nature (London) **355:**409–415.
54. **Salama, N. R., and R. W. Schekman.** 1995. The role of coat proteins in the biosynthesis of secretory proteins. Curr. Opin. Cell Biol. **7:**536–543.
55. **Smith, J. J., R. K. Szilard, M. Marelli, and R. A. Rachubinski.** 1997. The peroxin Pex17p of the yeast *Yarrowia lipolytica* is associated peripherally with the peroxisomal membrane and is required for the import of a subset of matrix proteins. Mol. Cell. Biol. **17:**2511–2520.
56. **Szilard, R. K., V. I. Titorenko, M. Veenhuis, and R. A. Rachubinski.** 1995. Pay32p of the yeast *Yarrowia lipolytica* is an intraperoxisomal component of the matrix protein translocation machinery. J. Cell Biol. **131:**1453–1469.
57. **Thieringer, R., H. Shio, Y. S. Han, G. Cohen, and P. B. Lazarow.** 1991. Peroxisomes in *Saccharomyces cerevisiae*: immunofluorescence analysis and import of catalase A into isolated peroxisomes. Mol. Cell. Biol. **11:**510–522.
58. **Titorenko, V. I., G. A. Eitzen, and R. A. Rachubinski.** 1996. Mutations in the *PAY5* gene of the yeast *Yarrowia lipolytica* cause the accumulation of multiple subpopulations of peroxisomes. J. Biol. Chem. **271:**20307–20314.
59. **Titorenko, V. I., and R. A. Rachubinski.** Submitted for publication.
60. **Walton, P. A., S. J. Gould, R. A. Rachubinski, S. Subramani, and J. R. Feramisco.** 1992. Transport of microinjected alcohol oxidase from *Pichia pastoris* into vesicles in mammalian cells: involvement of the peroxisomal targeting signal. J. Cell Biol. **118:**499–508.
61. **Wuestehube, L. J., R. Duden, A. Eun, S. Hamamoto, P. Korn, R. Ram, and R. Schekman.** 1996. New mutants of *Saccharomyces cerevisiae* affected in the transport of proteins from the endoplasmic reticulum to the Golgi complex. Genetics **142:**393–406.
62. **Wuestehube, L. J., and R. Schekman.** 1993. Selection and screening for yeast secretory mutants. Methods Mol. Genetics **1:**88–106.